Part IV
Radioactivity in Foods and Internal Exposure

Chapter 14
Radionuclides Behavior in Fruit Plants

Franca Carini, Massimo Brambilla, Nick G. Mitchell, and Hirofumi Tsukada

Abstract This paper summarizes research carried out on fruits by the Università Cattolica del Sacro Cuore (UCSC) in Piacenza, Italy. Among the fruit crops studied, strawberry, blackberry, grapevine, apple, pear, and olive, research on strawberry and blackberry was funded by the Food Standard Agency (UK). Fruit plants were grown in pots, kept under tunnels or in open field, and contaminated with ^{134}Cs and ^{85}Sr via leaves or via soil. Interception in strawberry plants ranges 39–17 % for ^{134}Cs, from anthesis (April) to predormancy (November). Leaf-to-fruit translocation occurs to a greater extent for ^{134}Cs than for ^{85}Sr. The distribution of contamination in fruit crops is an element-specific process: ^{134}Cs is preferentially allocated to fruits and ^{85}Sr to leaves. However, the activity in leaves is also species-specific: fruit species show different leaf-to-fruit translocation. Results on apple, pear, and grape crops indicate that the highest transfer from leaf to fruit occurs in apple crops. Olive plants also show ^{134}Cs translocation from leaves to trunks. Grapevines grown on mineral soil show a root uptake higher for ^{85}Sr than for ^{134}Cs, while strawberries grown on a peat substrate show a root uptake higher for ^{134}Cs than for ^{85}Sr. Rinsing directly contaminated fruits removes ^{85}Sr (36 %) to a greater degree than ^{134}Cs (24 %). Transfer to olive oil is low. A 57 % of ^{134}Cs is transferred from grapes to white wine.

F. Carini (✉)
Institute of Agricultural and Environmental Chemistry, Università Cattolica del Sacro Cuore, Via Emilia Parmense 84, I-29122 Piacenza, Italy
e-mail: fcarini33@gmail.com

M. Brambilla
Institute of Agricultural and Environmental Chemistry, Università Cattolica del Sacro Cuore, Via Emilia Parmense 84, I-29122 Piacenza, Italy

Consiglio per la ricerca in agricoltura e l'analisi dell'economia agraria (CRA), Unità di Ricerca per l'Ingegneria Agraria (CRA-ING), Laboratorio di Ricerca di Treviglio, Via Milano, 43, 24047 Treviglio, BG, Italy

N.G. Mitchell
Grant Harris Limited, PO Box 107, Haslemere, Surrey, GU27 9EF, UK

H. Tsukada
Institute of Environmental Radioactivity, Fukushima University, 1 Kanayagawa, Fukushima-shi, Fukushima 960-1296, Japan

T. Takahashi (ed.), *Radiological Issues for Fukushima's Revitalized Future*,
DOI 10.1007/978-4-431-55848-4_14

Keywords ^{134}Cs • ^{85}Sr • Fruits • Interception • Leaf-to-fruit translocation • Soil-to-fruit transfer • Wine-making • Food processing

14.1 Introduction

Radioactive contamination of the agricultural environment and the transfer of radionuclides through the food chain, as a consequence of a nuclear release, may require measures to protect human health and the environment. Understanding the behaviour of radionuclides in these situations is crucial if these measures are to be effective.

There are relatively few radioecological studies of fruit crops, which is surprising given that they contribute about 8 % of world food production and have a high economic value [1]. The fate of radionuclides in fruit systems is affected by a combination of biological, chemical, and physical processes and is sensitive to the timing of contamination relative to plant growth.

Contamination of fruits following an airborne release can occur from direct deposition of radionuclides onto the fruit surface, from deposition onto other above-ground parts of the plant, or after deposition onto soil. The relative contribution of these processes depends on many variables, such as the radionuclide involved, the plant species, the plant phenological stage at time of deposition, and the soil type. This topic was discussed under the IAEA BIOMASS program [2] and further updated in IAEA TRS 472 [3] and the accompanying TECDOC-1616 [4].

Various projects on fruit production systems have been carried out by the Università Cattolica del Sacro Cuore (UCSC) in Piacenza, Italy. Among the fruit crops studied were: strawberry, blackberry, grapevine, apple, pear, and olive. These studies considered plants grown in pots, kept under tunnels or in open field, and contaminated with ^{134}Cs and ^{85}Sr via aboveground plant parts or via soil. Research on strawberry and blackberry was funded by the Food Standard Agency (UK) and carried out as a collaborative project between Mouchel (UK) and the UCSC [5]. The objective of these projects was to understand the main processes that lead to fruit contamination in the short term after deposition. Processes of interception, leaf-to-fruit translocation and soil-to-fruit transfer are discussed in the following, as well as processing activities associated with fruits after harvest, such as pressing olives to produce oil and grapes for wine-making. Selected results from this research are compared and summarized in this paper.

14.2 Interception

Results are presented on interception by strawberry plants, *Fragaria x ananassa* Duchesne. Strawberry is a herbaceous perennial member of the rose family (Rosaceae). The study used June bearer plants, cultivar Miss, which are

representative of commercial production in Italy. Young strawberry plants are transplanted at the end of July, develop flower buds in the autumn, lose all old leaves at the resumption of growth (in March), flower in the spring, and produce a single crop from early May to June. After harvest, plants are removed and replaced by new plants.

The aboveground part of different sets of strawberry plants was contaminated with ^{134}Cs and ^{85}Sr at various phenological stages: predormancy (November), preanthesis (early April), anthesis (end of April), and beginning of ripening (May). The fresh weight activity (Bq per kg fresh weight), biomass (g dry weight per plant), and leaf area (cm^2 per plant) were measured for each of the four replicates. Intercepted activity (%) was calculated from the ratio of activity deposited on the plant per total activity applied:

$$I\,(\%) = \frac{\text{Bq in plant component}}{\text{Bq applied} \cdot \text{plant}^{-1}} \times 100$$

Results for ^{134}Cs are reported in Fig. 14.1.

The results show that interception for ^{134}Cs is highest at anthesis (the period of flower development that starts with the opening of the flower buds), 39 %, and

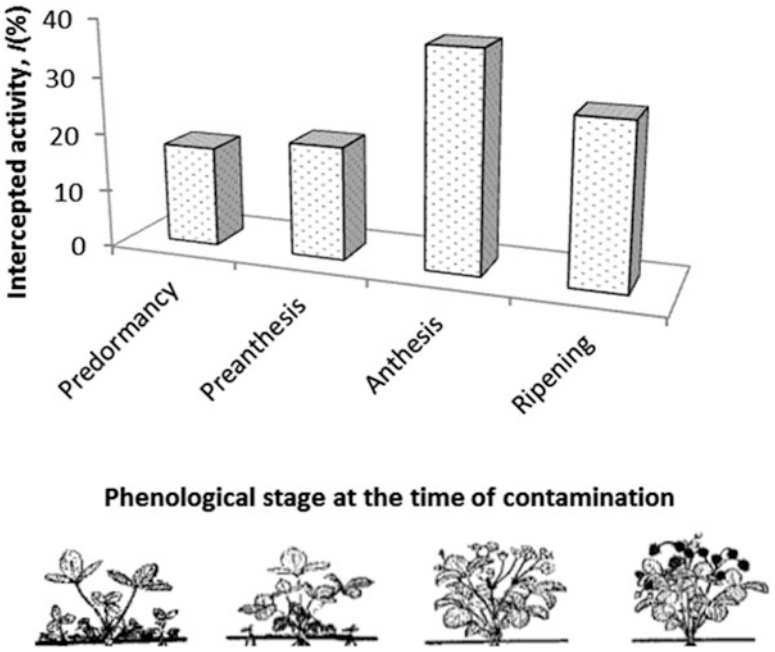

Fig. 14.1 ^{137}Cs intercepted by strawberry plants after deposition at different phenological stages: predormancy, preanthesis, anthesis, and ripening. I(%) is expressed as (Bq in plant component per Bq sprinkled $\cdot$ plant^{-1}) $\cdot$ 100

lowest at predormancy, 17 % [6]. Fruits, when present, have a lower interception capability than leaves, even if crop management, aimed at increasing the exposure of fruits to light, favors direct deposition and interception by fruit.

In a number of experimental studies, the interception of wet deposited radioactivity was found to be positively correlated with the leaf area and/or the dry biomass of the crop [7]. However, in the study described here there was no correlation between the interception capacity of strawberry plants and leaf area or biomass. Interception, at the growth stages considered, seems rather to be affected by variables such as the leaf senescence and the posture and physical orientation of leaves. A similar result was obtained contaminating tomato plants at two growing stages, demonstrating that an increase in the leaf surface area at later growing stages does not necessarily imply an increase in the level of interception of wet deposition [8].

Renaud and Gonze [9], studying the ^{134}Cs contamination of orchard fruits in Japan in 2011, observed that some correlation exists between cesium concentration in fruits, at first harvest, and ground surface deposit. They calculated the aggregated transfer factors, T_{ag}, expressed in $\mathrm{Bq \cdot kg^{-1}}$ of fresh fruit per $\mathrm{Bq \cdot m^{-2}}$ deposited on the ground surface. They observed that T_{ag} values of apricot samples were apparently higher when collected in low-elevation coastal areas (i.e., in Minamisoma-shi and Soma-shi municipalities, located to the North of the nuclear site, and Mito-shi to the South in Ibaraki Prefecture) than those collected from sites in mountainous areas. They suggested these differences were due to the stage of the vegetative cycle, as flowering would have occurred earlier in coastal regions than in inland elevated areas, resulting in greater transfer [9]. Similarly, the radiocesium activities of the foliar parts of woody species, 5 months after the Fukushima accident, were higher in evergreen species than in deciduous species, because the foliar parts of evergreen species (leaves from previous year) were present at the time of fallout but those of the deciduous species were not [10].

14.3 Leaf-to-Fruit Translocation

Fruits can receive radionuclides via translocation from contaminated aerial parts of plants, the most receptive of which, when present, is foliage. Leaf-to-fruit translocation has been studied in apple, pear, grapes, olives, blackberry, and strawberry plants, after contamination of leaves by wet deposition of ^{134}Cs and ^{85}Sr in open field conditions [6, 11–14]. The activity in fruits (Bq per kg fresh weight) was measured at ripening. Leaf-to-fruit translocation coefficients were calculated to represent the share of ^{134}Cs or ^{85}Sr activity found in fruits at ripening. Translocation coefficients, TC(%), are expressed as:

$$TC\,(\%) = \frac{\mathrm{Bq \cdot kg^{-1}\,fresh\ weight\ fruit}}{\mathrm{Bq\ \ intercepted \cdot plant^{-1}}} \times 100$$

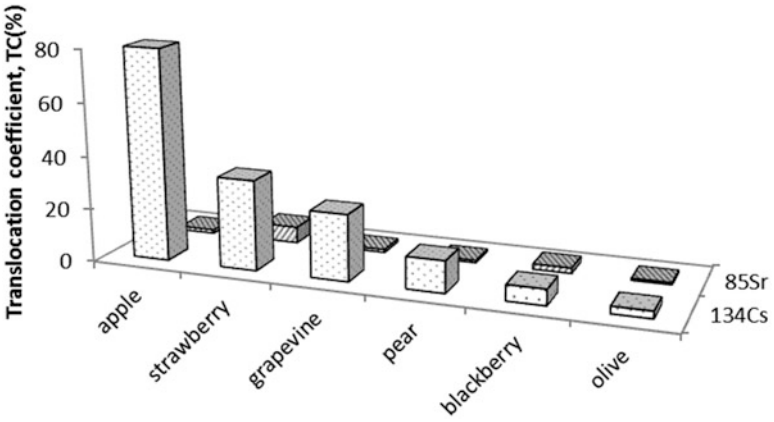

Fig. 14.2 Leaf-to-fruit translocation of ^{134}Cs and ^{85}Sr in various fruit crops. Translocation coefficients, TC(%), are expressed as (Bq kg^{-1} fresh weight fruit per Bq intercepted $plant^{-1}$) · 100

Results, reported in Fig. 14.2, indicate that the leaf-to-fruit TCs are on average one order of magnitude higher for ^{134}Cs than for ^{85}Sr in all fruit crops studied. This result is expected on the basis of greater foliar absorption of Cs^+ than Sr^{2+} [15] and greater mobility, after absorption, in the phloem of monovalent ions than divalent ones [16, 17]. This makes the fruits sinks for cesium.

Differences in the process of foliar absorption and leaf-to-fruit translocation also exist between fruit species. Our results showed TCs for ^{134}Cs declined in the following order: apple trees, strawberry, grapevine, pear, blackberry, and olive plants (Fig. 14.2). A different trend was observed after the Chernobyl accident, in 1986, when Baldini et al. [18] found greater TCs for grapevine and peach than for apple and pear, and ascribed the differences to the more active metabolism of grapevine and peach.

However leaf-to-fruit translocation is also highly dependent on the time at which contamination occurs during the growth period of crops [19] and this can explain the results under different experimental conditions. In this regard, plants of strawberry and blackberry were contaminated with ^{134}Cs and ^{85}Sr via leaves at different growing stages: predormancy (November for strawberry and October for blackberry), anthesis (April for strawberry and May for blackberry), and beginning of ripening (May for strawberry and June for blackberry) [5, 6, 14, 20, 21]. Ripe fruits were picked and analyzed.

The growth cycle of strawberry plants was described earlier and a short description of blackberry plants is given in the following.

Blackberry is a bush plant, widespread in Northern Europe, with a perennial root apparatus and a biannual aerial part: the canes dry after having borne fruits. Blossoming is scalar, lasting up to 5–6 weeks. As a consequence, ripening is also very prolonged, from mid-July onward. The consumption of blackberry fruit is common particularly in northern countries, and can play a role in the diet of particular population groups.

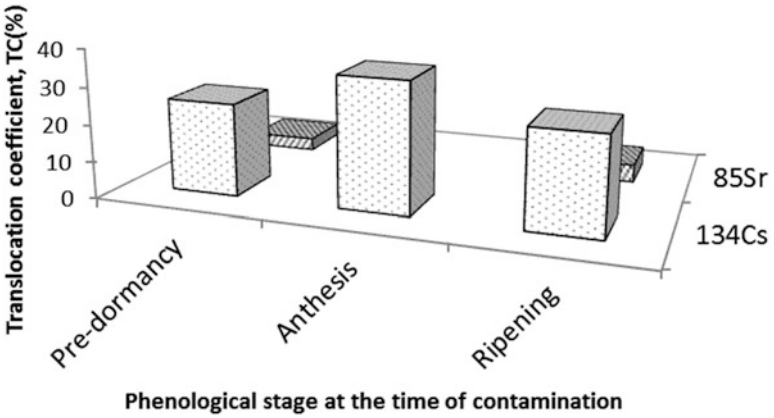

Fig. 14.3 Leaf-to-fruit translocation in strawberry: ^{134}Cs and ^{85}Sr activity translocated in fruit after leaf deposition at different phenological stages: predormancy, anthesis, and ripening. Translocation coefficients, TC(%), are expressed as (Bq kg^{-1} fresh weight fruit per Bq intercepted plant^{-1}) · 100

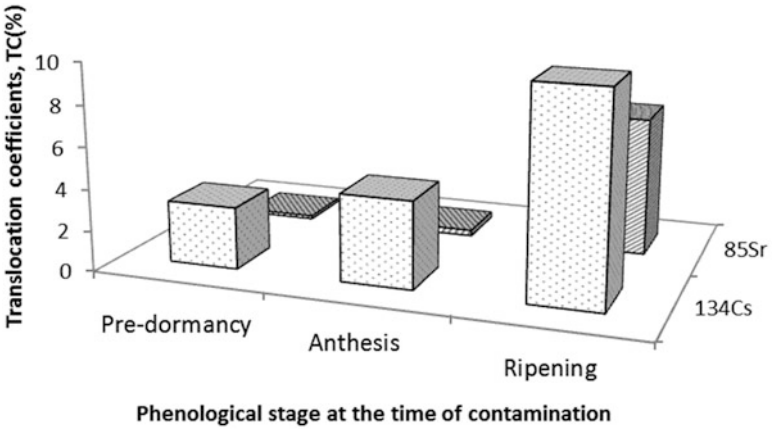

Fig. 14.4 Leaf-to-fruit translocation in blackberry: ^{134}Cs and ^{85}Sr activity translocated in fruit after leaf deposition at different phenological stages: predormancy, anthesis, and ripening. Translocation coefficients, TC(%), are expressed as (Bq kg^{-1} fresh weight fruit per Bq intercepted plant^{-1}) · 100

The activity (Bq per kg fresh weight) of fruits was determined and TCs(%) calculated; results are shownin Figs. 14.3 and 14.4 for strawberry and blackberry, respectively. The objective of this study was to show the dependence of plant contamination on the time of the year when the deposition occurs, referred to as seasonality by Aarkrog [22]. In strawberry, leaf-to-fruit translocationis greatest at

anthesis, following the pattern observed for interception (Figs. 14.1 and 14.3). This result supports the hypothesis that interception is also affected by leaf age and by the metabolic activity of the plant. Increasing leaf age seems to reduce the absorption of radionuclides [23, 24].

When deposition occurs at predormancy, strawberry plants present well-developed leaves to aerial deposition, even if some are aging at this stage of the growing cycle. The plants have also developed flower buds for the following spring. A proportion of the radionuclides intercepted by, and absorbed into the leaves, is remobilized and translocated to the storage organs (roots and crowns) before leaf drop. Remobilization of ^{134}Cs is presumably higher than that of ^{85}Sr, given its higher mobility in the phloem. A few months later, the activity in ripe fruits is one order of magnitude greater for ^{134}Cs than for ^{85}Sr, an indication of the greater translocation of ^{134}Cs than ^{85}Sr from roots and crowns to fruits (Fig. 14.3).

In blackberry plants, the leaf-to-fruit translocation is greatest when foliar contamination occurs at ripening, and is one order of magnitude higher for ^{134}Cs than for ^{85}Sr (Fig. 14.4). When blackberry plant contamination occurs in Autumn, at predormancy, the plant system loses 60 % of the intercepted activity through dead leaves during Winter. A remaining 20 % is released into the soil and the environment. Fruit activity at harvest will be the result of retranslocation from roots and shoots (the storage organs) toward the fruits.

Recent observations after the Fukushima accident provide evidence that translocation to fruit does occur from leaf and bark, the amount of translocation differs between plant types, and that translocation is very sensitive to plant growth stage at the time of deposition [9, 25–27]. Another process that can contribute to fruit activity, ascertained by various authors after the Fukushima accident, is the secondary contamination, resulting from weathering, by the action of wind and rain [10, 27–30 cited by 28].

14.4 Soil-to-Fruit Transfer

Soil-to-fruit transfer was studied for grapevines, blackberry, and strawberry plants grown in pots [5, 11, 14, 21]. The crops were grown under different conditions using soils most suited to their cultivation. Data are not therefore comparable and are discussed separately as follows.

Root uptake for blackberry and strawberry plants was studied at two phenological stages: predormancy and anthesis. Results are presented as transfer factors, expressed as in IAEA [4]:

$$F_v = \frac{\text{Bq} \cdot \text{kg}^{-1} \text{ fresh weight fruit}}{\text{Bq} \cdot \text{kg}^{-1} \text{ dry soil}}$$

14.4.1 Grapevines

Two-year-old grapevines, variety Pinot Blanc, were grown in pots of 10 L capacity and kept in open field conditions. Pots were filled with a substrate of mineral soil (70 %) and sand (30 %). The mineral soil is moderately acidic (pH in H_2O 5.7), with low organic matter content (OM = 1.6 %) and low cation exchange capacity (CEC = 13.2 $cmol_{(+)}$/kg). The substrate of each pot was contaminated by moistening the surface with 250 mL of an aqueous solution containing 5305 kBq of ^{134}Cs and 2063 kBq of ^{85}Sr per pot after the fruit setting, at the beginning of July.

The objective of this study was to assess the transfer of ^{134}Cs and ^{85}Sr to fruit and other parts of the vine. At ripening, 60 days after soil contamination, F_v from soil to the whole plant was greater for ^{85}Sr than for ^{134}Cs, but while ^{85}Sr concentrates mainly in leaves and shoots, ^{134}Cs is redistributed throughout the plant. As a result, ^{134}Cs and ^{85}Sr F_v (mean ± standard error) in grapes are similar: $(8.0 \pm 0.9) \cdot 10^{-2}$ and $(6.6 \pm 1.2) \cdot 10^{-2}$, respectively [12].

14.4.2 Blackberry Plants

Two–year-old blackberry plants, cultivar Chester Thornless, were grown in 20 L capacity pots, filled with a mixture of peat (55 % of the total substrate), pumice, and compost. This is a medium with pH in H_2O 6.6, rich in organic matter (39.1 %), and with a high CEC (33.2 $cmol_{(+)}$/kg). Different sets of plants were contaminated in Autumn, at predormancy (October), and in Spring, at the beginning of anthesis (May). The soil surface was moistened with 800 mL of an aqueous solution containing 298 kBq of ^{134}Cs and 1921 kBq of ^{85}Sr per pot. The experiment lasted for 2 years following the growth cycle of this crop. The radionuclide content of fruit was determined at ripening, 276 or 74 days, respectively, after soil contamination.

The F_v are reported in Fig. 14.5. The F_v for ^{85}Sr is one order of magnitude greater than for ^{134}Cs and reflects the behavior of these radionuclides in mineral rather than organic soils [31]. The ratio of ^{85}Sr to ^{134}Cs in fruit was 12:1.

As for the phenological stages, a significant difference is shown ($p < 0.05$) for ^{85}Sr F_v mean and standard error: $(7.9 \pm 0.2) \cdot 10^{-1}$ at predormancy and $(5.9 \pm 0.2) \cdot 10^{-1}$ at anthesis; no significant difference is shown for ^{134}Cs: $(7.7 \pm 0.2) \cdot 10^{-2}$, at both plant stages.

14.4.3 Strawberry

Strawberry plants,cultivar MISS, were grown in 4.5 L capacity pots filled with peat, the normal substrate under horticultural growing conditions. Peat characteristics

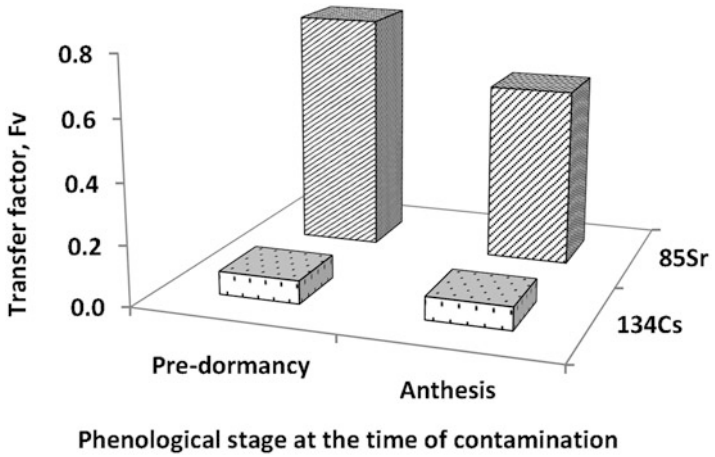

Fig. 14.5 Soil-to-fruit transfer factors F_v of ^{134}Cs and ^{85}Sr to blackberry following soil contamination at two phenological stages: predormancy and anthesis. F_v are expressed as (Bq kg^{-1} fresh weight fruit per Bq kg^{-1} dry soil)

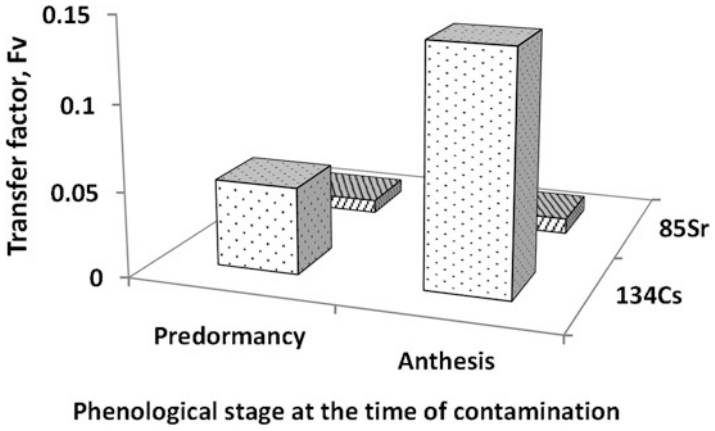

Fig. 14.6 Soil-to-fruit transfer factors F_v of ^{134}Cs and ^{85}Sr to strawberry following soil contamination at two phenological stages: predormancy and anthesis. F_v are expressed as (Bq kg^{-1} fresh weight fruit per Bq kg^{-1} dry soil)

were: a moderate acid pH (5.7), high OM (48.1 %), and high CEC (111.5 cmol$_{(+)}$/kg). The soil surface of each pot was moistened with 250 mL of an aqueous solution containing 74.8 kBq of ^{134}Cs and 91.6 kBq of ^{85}Sr at two phenological stages: predormancy (November) and anthesis (April). The experiment lasted for 3 years.

The radionuclide content of fruit was determined at ripening, 200 and 70 days respectively, after soil contamination. F_v are reported in Fig. 14.6 and show greater root uptake for ^{134}Cs, $(5.1 \pm 0.3) \cdot 10^{-2}$ at predormancy and $(1.4 \pm 0.1) \cdot 10^{-1}$ at

anthesis, than for ^{85}Sr, $(7.8 \pm 0.9) \cdot 10^{-3}$ and $(9.2 \pm 1.6) \cdot 10^{-3}$, respectively. The ratio of ^{134}Cs to ^{85}Sr in fruit was 15:1.

The high organic matter content of the peat substrate, responsible for a large part of the CEC, reduces ^{134}Cs fixation on clay minerals, leaving it more available for root uptake, as highlighted by Nisbet and Shaw [31]. In contrast, it has been demonstrated that the organic matter of peat may form complex compounds with ^{85}Sr, reducing its availability to plants.

Differences in transfer to fruit after soil contamination at different phenological stages is apparent only for ^{134}Cs: F_v, are three times higher after contamination at anthesis than at predormancy (Fig. 14.6), the opposite was observed for blackberry fruits (Fig. 14.5).

Results on soil-to-plant transfer for blackberry and strawberry plants highlight time-dependent changes of root uptake following acute soil deposition during plant growth, as discussed by Choi [32]. These changes are more significant for an annual plant like strawberry, than for a perennial plant (with a perennial root apparatus) like blackberry and are more apparent for those radionuclides with the greatest transfer: ^{134}Cs on peat and ^{85}Sr on mineral soil.

14.5 Food Processing

Food processing losses can vary considerably depending on the type of radionuclide and between processes at the industrial and domestic scales. Rinsing directly contaminated apples (Golden Delicious) and grapes (Chardonnay) with tap water, simulating common domestic practice before consumption, removes ^{85}Sr to a greater degree than ^{134}Cs [13]. The processing factor P_f [3], called food processing retention factor, f_{fp}, in ICRU 65 [33], is the ratio of the radionuclide activity concentrations in the food after and before processing:

$$Pf = \frac{\text{Bq} \cdot \text{kg}^{-1} \text{ processed food}}{\text{Bq} \cdot \text{kg}^{-1} \text{ raw food}}$$

In our observations, it corresponds to 0.7 for ^{85}Sr and 0.8 for ^{134}Cs.

14.5.1 Wine-Making

A study of Pinot Blanc grapes, contaminated following an application of ^{134}Cs to leaves at the beginning of ripening, replicated the wine-making process on a small scale under laboratory conditions. Grapes were picked at the ripening stage, 35 days after contamination, analyzed for ^{134}Cs and squeezed to separate skin, pulp, and seeds from must (the juice extracted from grapes). The processing factor, P_f, for must was 0.94.

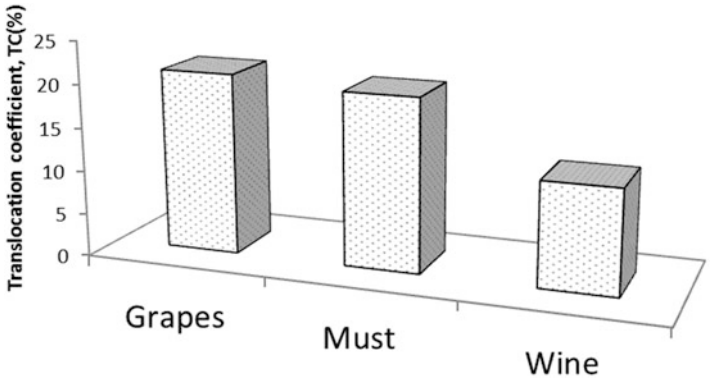

Fig. 14.7 Translocation coefficients, TC(%), from leaf to grapes, must, and wine for ^{134}Cs, expressed as (Bq kg^{-1} fresh weight per Bq intercepted plant^{-1}) · 100

Must was then inoculated (under controlled conditions) with $2.8 \cdot 10^5$ cells of the yeast Saccaromyces cerevisiae · mL^{-1} to begin the fermentation process. The must was fermented at 25 °C until constant weight was achieved. During the fermentation process, sugar changes into alcohol releasing CO_2 with a loss of weight:

$$C_6H_{12}O_6 \rightarrow 2\,(CH_3CH_2OH) + 2(CO_2) + \text{energy}$$

At the end of the process, the fermented must was filtered to remove any sediment. The ^{134}Cs content of wine corresponded to 61 % of the must activity (Fig. 14.7). Several different wine-making processes are practiced in industry, but all entail filtration, which is also carried out for home-made wine.

In practical situations the activity in wine can be quantified by the food processing factor P_f, if the activity of grapes is known, as follows: $P_f = (\text{Bq} \cdot \text{kg}^{-1}$ wine) per (Bq · kg^{-1} grapes). In this experimental study P_f for ^{134}Cs from grapes to wine was of 0.57. From the recent literature, the transfer of stable ^{133}Cs from rice to Japanese sake has been reported by Okuda et al. [34]. The authors calculated a P_f value of 0.04 from brown rice grains to sake.

14.5.2 Olive-Oil-Making

A second study was carried out using olive plants, *Gentile di Chieti*, contaminated via leaves with ^{134}Cs and ^{85}Sr at the beginning of ripening (at the end of September) [35]. At ripening, 10 days after contamination, olives were picked, analyzed for ^{134}Cs and ^{85}Sr, crushed by a mill, and pressed using a hydraulic jack, producing a fluid comprising oil, wastewater, and solid impurities. The oil was then separated from wastewater and solids by centrifugation. TCs were calculated for leaf-to-olives, leaf-to-wastewater, and leaf-to-oil. Results are shown in Fig. 14.8.

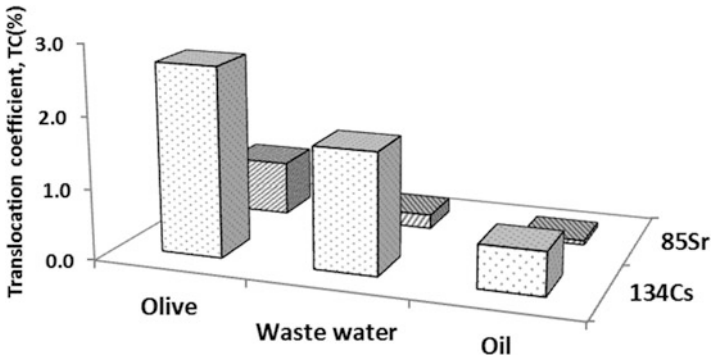

Fig. 14.8 Translocation coefficients, TC(%), from leaf to olive, wastewater, and oil, expressed as (Bq kg^{-1} fresh weight per Bq intercepted $plant^{-1}$) · 100

Only a small fraction of ^{134}Cs in fruit is transferred to oil. ^{85}Sr transfer to oil is not significant. P_f in this research, expressed as (Bq · kg^{-1} oil) per (Bq · kg^{-1} olives), gives values of 0.23 for ^{134}Cs and of 0.08 for ^{85}Sr, indicating that 77 % of ^{134}Cs and 92 % for ^{85}Sr are removed in the process of oil-making. Other studies on olive plants contaminated via soil report that a significant soil-to-fruit transfer of ^{134}Cs may occur, but no transfer to oil is detected [36]. Results from Cancio et al. [37] show that processing into olive oil removes ∼90 % of the ^{134}Cs contamination initially contained in olive fruit. The P_f for olive oil obtained from data reported in the IAEA TRS 472 gives a value of 0.65 for ^{134}Cs [3].

14.6 Conclusions

From research at UCSC carried out on various fruit plants concerning the behavior of ^{134}Cs and ^{85}Sr after aerial or soil contamination, the following conclusions can be drawn:

- Interception seems to be affected by variables such as leaf senescence and the posture and physical orientation of leaves, rather than by leaf area or biomass.
- Leaf-to-fruit translocation is always higher for ^{134}Cs than for ^{85}Sr . It is also affected by the metabolic activity of the plant and by the phenological stage at time of contamination. The reproductive stages, like anthesis, lead to greater contamination of fruit.
- Soil-to-fruit transfer depends on the growing substrate. It is greater for ^{85}Sr on mineral soils, and greater for ^{134}Cs on peaty soils. Time-dependent changes of soil-to-fruit transfer following acute deposition are not insignificant in annual plants.
- The process of wine-making removes more than 40 % of ^{134}Cs present in grapes; that of oil-making removes about 75 % of ^{134}Cs and 90 % of ^{85}Sr in olives.

References

1. Salunkhe DK, Deshpande SS (1988) In: Salunkhe DK, Deshpande SS (eds) Foods of plant origin: production, technology and human nutrition. Van Nostrand Reinhold, New York, pp 1–5
2. International Atomic Energy Agency (2003) Modelling the transfer of radionuclides to fruit. Report of the fruits working group of BIOMASS theme 3, BIOsphere Modelling and ASSessment Programme, IAEA-BIOMASS-5, Vienna
3. International Atomic Energy Agency (2010) Handbook of parameter values for the prediction of radionuclide transfer in terrestrial and freshwater environments. Technical reports series no. 472. IAEA-TRS 472, Vienna
4. International Atomic Energy Agency (2009) Quantification of radionuclide transfer in terrestrial and freshwater environments for radiological assessments. IAEA-TECDOC-1616, Vienna
5. Food Standards Agency (2002) Experimental and modelling study on strawberry and blackberry, Draft final report, Mouchel Consulting Limited, Ref. 48100, Surrey, p 114
6. Carini F, Brambilla M, Ould-Dada Z, Mitchell NG (2003) 134Cs and 85Sr in strawberry plants following wet aerial deposition. J Environ Qual 32:2254–2264
7. Pröhl G, Hoffman FO (1996) Radionuclide interception and loss processes in vegetation. In: Modelling of radionuclide interception and loss processes in vegetation and of transfer in semi-natural ecosystems. Second report of the VAMP terrestrial working group, IAEA-TECDOC-857, Vienna, pp 9–48
8. Brambilla M, Fortunati P, Carini F (2002) Foliar and root uptake of 134Cs, 85Sr and 65Zn in processing tomato plants (Lycopersicon esculentum Mill.). J Environ Radioact 60:351–363
9. Renaud P, Gonze M-A (2014) Lessons from the Fukushima and Chernobyl accidents concerning the 137Cs contamination of orchard fresh fruits. Radioprot 49(3):169–175
10. Yoshihara T, Matsumura H, Hashida S-N, Nagaoka T (2013) Radiocesium contaminations of 20 wood species and the corresponding gamma-ray dose rates around the canopies at 5 months after the Fukushima nuclear power plant accident. J Environ Radioact 115:60–68
11. Carini F, Anguissola Scotti I, Montruccoli M, Silva S (1996) 134Cs foliar contamination of vine: translocation to grapes and transfer to wine. In: Gerzabek MH (ed) International symposium of the Austrian Soil Science Society: ten years terrestrial radioecological research following the Chernobyl accident, Vienna, 22–24 aprile, pp 163–169
12. Carini F, Lombi E (1997) Foliar and soil uptake of 134Cs and 85Sr by grape vines. Sci Total Environ 207:157–164
13. Carini F, Anguissola Scotti I, D'Alessandro PG (1999) 134Cs and 85Sr in fruit plants following wet aerial deposition. Health Phys 77(5):520–529
14. Fortunati P, Brambilla M, Carini F (2002) 134Cs and 85Sr in blackberry plants. Radioprotection – Colloques, Numéro spécial. In: Bréchignac F (ed) Proceedings of the international congress "The Radioecology – Ecotoxicology of Continental and Estuarine Environments, ECORAD 2001", Aix-en-Provence, 3–7 Sept 2001, vol 37, C1-547–552
15. Swietlik D, Faust M (1984) Foliar nutrition of fruit crops. Hortic Rev 6:299–301
16. Russel RS (1965) An introductory review: interception and retention of airborne material on plants. Health Phys 11:1305–1315
17. Marschner H (2002) Mineral nutrition in higher plants, 2nd edn. Academic, London
18. Baldini E, Bettoli MG, Tubertini O (1987) Effects of the Chernobyl pollution on some fruit trees. Adv Hortic Sci 1(2):77–79

19. Simmonds JR (1985) The influence of season of the year on the transfer of radionuclides to terrestrial foods following an accidental release to atmosphere. National Radiological Protection Board, NRPB-M121, Chilton Didcot
20. Fortunati P, Brambilla M, Carini F (2003) Trasferimento suolo-pianta di ^{134}Cs e ^{85}Sr in mora (Rubus fruticosus). Atti del Convegno annuale La conservazione della risorsa suolo. Piacenza, 8–10 giugno 2002. Bollettino della Società Italiana della Scienza del Suolo 52(1–2):363–372
21. Fortunati P, Brambilla M, Carini F (2003b) ^{134}Cs and ^{85}Sr in blackberry plants. In: Proceedings of the 7th international conference on the biogeochemistry of trace elements, 15–19 Jun 2003, vol 2. Slu, Uppsala, pp 376–377
22. Aarkrog A (1992) Seasonality. In: Modelling of resuspension, seasonality and losses during food processing. First report of the VAMP terrestrial working group, International Atomic Energy Agency, IAEA-TECDOC-647, Vienna, pp 61-96
23. Aarkrog A (1969) On the direct contamination of rye, barley, wheat and oats with 85Sr, 134Cs, 54Mn and 141Ce. Radiat Bot 9:357–366
24. Fortunati P, Brambilla M, Speroni F, Carini F (2004) Foliar uptake of ^{134}Cs and ^{85}Sr in strawberry as function by leaf age. J Environ Radioact 71/2:187–199
25. Nihei N (2013) Radioactivity in agricultural products in Fukushima. Chapter 8. In: Nakanishi TM, Tanoi K (eds) Agricultural implications of the Fukushima nuclear accident. Graduate School of Agricultural and Life Sciences, The University of Tokyo. Springer Open, Tokyo, pp 73–85. doi:10.1007/978-4-431-54328-2_14
26. Tagami K, Uchida S (2015) Effective half-lives of 137Cs from persimmon tree tissue parts in Japan after Fukushima Dai-ichi nuclear power plant accident. J Environ Radioact 141:8–13
27. Takata D (2013) Distribution of radiocesium from the radioactive fallout in fruit trees. Chapter 14. In: Nakanishi TM, Tanoi K (eds) Agricultural implications of the Fukushima nuclear accident. Graduate School of Agricultural and Life Sciences, The University of Tokyo. Springer Open, Tokyo, pp 143–162. doi:10.1007/978-4-431-54328-2_14
28. Toshihiro Yoshihara, Shin-nosuke Hashida, Kazuhiro Abe, Hiroyuki Ajito (2014a) A time dependent behavior of radiocesium from the Fukushima-fallout in litterfalls of Japanese flowering cherry trees. J Environ Radioact 127:34–39. doi:10.1016/j.jenvrad.2013.09.007
29. Tagami K, Uchida S, Ishii N, Kagiya S (2012) Translocation of radiocesium from stems and leaves of plants and the effect on radiocesium concentrations in newly emerged plant tissues. J Environ Radioact 111:65–69
30. Nakanishi TM, Kobayashi NI, Tanoi K (2012) Radioactive cesium deposition on rice, wheat, peach tree and soil after nuclear accident in Fukushima. J Radioanal Nucl Chem. doi:10.1007/s10967-012-2154-7 (Published Online)
31. Nisbet AF, Shaw S (1994) Summary of a 5-year lysimeter study on the time-dependent transfer of 137Cs, 90Sr, 239,240Pu and 241Am to crops from three contrasting soil types: 1. Transfer to the edible portion. J Environ Radioact 23(1):1–17
32. Choi YH (2009) Root uptake following acute soil deposition during plant growth. In: Quantification of radionuclide transfer in terrestrial and freshwater environments for radiological assessments. IAEA-TECDOC-1616, Vienna, pp 253–258.
33. International Commission on Radiation Units and Measurements, ICRU Report 65, (2001) Quantities, units and terms in radioecology. J ICRU 1(2):15
34. Masaki Okuda, Midori Joyo, Masafumi Tokuoka, Tomokazu Hashiguchi, Nami Goto-Yamamoto, Hiroshi Yamaoka, Hitoshi Shimoi (2012) The transfer of stable 133Cs from rice to Japanese sake. J Biosci Bioeng 114(6):600–605
35. Aquilano C (2001) Traslocazione di ^{134}Cs e ^{85}Sr in piante di olivo e nell'olio. Tesi di laurea. Università Cattolica del Sacro Cuore, Piacenza
36. Skarlou V, Nobeli C, Anoussis J, Haidouti C, Papanicolaou E (1999) Transfer factors of 134Cs for olive and orange trees grown on different soils. J Environ Radioact 45(2):139–147
37. Cancio D, Maubert H, Rauret G, Colle C, Cawse PA, Grandison AS, Gutierrez P (1993) Transfer of accidentally released radionuclides in agricultural systems (TARRAS). In: CEC (ed) CEC Euratom radiation protection programme progress report 1990–1991 EUR 14927 DE/EN/FR, Luxembourg, pp 579–600

Chapter 15
Effect of Nitrogen Fertilization on Radiocesium Absorption in Soybean

Naoto Nihei, Atsushi Hirose, Mihoko Mori, Keitaro Tanoi, and Tomoko M. Nakanishi

Abstract Radioactive materials that were released during the nuclear accident contaminated the soil and agricultural products. It has become clear that potassium fertilization is effective for the reducing radiocesium concentrations in agricultural crops. However, apart from reports about potassium, few reports have examined how nitrogen (N), which has a large effect on crop growth, contributes to the radiocesium absorption. Focusing on this point, we studied the effect of nitrogen fertilizer on the radiocesium absorption in soybean seedlings. The concentration of radiocesium in the seed of soybean was higher in nitrogen-fertilized plants than in plants grown without fertilizer. The radiocesium concentration in the aboveground biomass increased as the amount of nitrogen fertilization increased. A comparison of the effects of the different forms of nitrogen treatment shows that the highest radiocesium concentration in the aboveground biomass occurred with ammonium sulfate (approximately 3.7 times the non-N), the next highest absorption occurred with ammonium nitrate (approximately 2.4 times the non-N treatment), followed by calcium nitrate (approximately 2.2 times the non-N treatment). Furthermore, the amount of radiocesium in soil extracts was highest with ammonium-nitrogen fertilization. Further study is required to clarify the factors that incur an increase in radiocesium concentration in response to nitrogen fertilization. Special care is required to start farming soybean on fallow fields evacuated after the accident or on fields where rice has been grown before, which tend to have higher available nitrogen than the regularly cultivated fields.

Keywords Radiocesium • Soybean • Nitrogen • Ammonium

N. Nihei (✉) • A. Hirose • M. Mori • K. Tanoi • T.M. Nakanishi
Graduate School of Agricultural and Life Science, The University of Tokyo, 1–1–1, Yayoi, Bunkyo-ku, Tokyo, Japan
e-mail: anaoto@mail.ecc.u-tokyo.ac.jp

T. Takahashi (ed.), *Radiological Issues for Fukushima's Revitalized Future*,
DOI 10.1007/978-4-431-55848-4_15

15.1 Introduction

The Great East Japan Earthquake occurred on March 11, 2011, and it was immediately followed by the accident at the Fukushima Daiichi Nuclear Power Plant, Tokyo Electric Power Company. Radiocesium, the dominant nuclide released during the accident, reached agricultural lands in Fukushima and its neighboring prefectures and contaminated the soil and agricultural products [1, 2]. To guarantee the safe consumption and handling of agricultural, livestock, forestry, and marine products, monitoring inspections were established [3]. According to these inspections [4–6] the ratio of samples exceeding the new standard value of radiocesium [7] (100 Bq kg^{-1}) were found to be 5.7 % for soybean, 2.6 % for rice, and 11 % for wheat in 2011; 2.6 % for soybean, 0.0007 % for rice, and 0 % for wheat in 2012; and 1.9 % for soybean, 0.0003 % for rice, and 0 % for wheat in 2013. The inspection results indicate that the ratio of soybean exceeding 100 Bq kg^{-1} was high compared with that for rice and wheat and that the tendency to decline was low compared with that for rice and wheat. To revitalize agriculture, Fukushima Prefecture has been promoting the decontamination of agricultural lands; consequently, it has implemented an increase in the exchangeable potassium content in soil used to grow rice to approximately 25 mg 100 g^{-1} (dry soil) or higher. This occurred because it recently became clear that potassium fertilization was effective for reducing the radiocesium concentration in agricultural crops [8, 9]. Nitrogen (N) has a large effect on crop growth, and some reports have suggested that it also promotes the radiocesium absorption [10, 11]. However, few studies have examined how nitrogen contributes to the radiocesium absorption in soybean apart from potassium.

For the recovery and revitalization of agricultural industries, the analysis of radiocesium absorption in soybeans is necessary. Focusing on this point, we studied the effect of nitrogen fertilizers on the radiocesium absorption in soybean seedlings.

15.2 Materials and Methods

We cultured soybean (*Glycine max*) in a greenhouse (experiment 1) and in a field (experiment 2). For experiment 1, nitrogen fertilizer in the form of ammonium sulfate was applied at two levels: 0.4 and 1.3 g per 1 L pot (hereafter low-N and high-N, respectively). The radiocesium activity of the soil which was taken in Fukushima in August 2012 was approximately 30 kBq kg^{-1}, exchangeable potassium was 13.4 mg 100 g^{-1} soil, and pH was 6.0. The plants were grown until maturity, and the seed was collected. For experiment 2, soybean was grown in Iitate Village, Fukushima Prefecture. The radiocesium of the field was approximately 13 kBq kg^{-1} (15-cm depth), exchangeable potassium was 15.8 mg 100 g^{-1}, and pH was 6.2. Nitrogen fertilizer in the form of ammonium nitrate was applied at three levels: 0, 50, and 100 kg ha^{-1} (hereafter non-N, low-N, and high-N, respectively). We sowed the seeds for experiment 2 on June 16, 2014, and collected the aboveground

biomass on September 2, 2014. Next, we studied the effect of the different forms of nitrogen treatment on radiocesium absorption by soybean seedling (experiment 3). Nitrogen was applied as calcium nitrate, ammonium nitrate, and ammonium sulfate at three levels: 0, 0.01, and 0.05 g per treatment (hereafter non-N, low-N, and high-N, respectively). We cultured soybean in a vessel ($6.5 \times 6.5 \times 6.5$ cm) for 18 days in a biotron (28 °C, 16 h light). We collected the aboveground biomass. Moreover, we studied radiocesium activity in soil extracts following nitrogen application (experiment 4). Nitrogen was applied to the soil at 0.5 g kg^{-1} as ammonium sulfate. We collected the soil after 1, 5, and 15 days, extracted it with 1 M calcium chloride, and then measured the radiocesium activity. We used soil sourced from the same batch in Experiment 1, 3, and 4. The radiocesium activities of all samples were measured using a sodium iodide scintillation counter (Aloka AM-300). In experiment 3, potassium, calcium, and magnesium concentrations in the soybean seedling were measured after acid decomposition using inductively coupled plasma optical emission spectrometry (ICP-OES) (PerkinElmer, Optima 7300).

15.3 Results

Figure 15.1 shows the effect of nitrogen fertilizer on radiocesium absorption by soybean. The concentrations of radiocesium in the seed (experiment 1) or the aboveground biomass (experiment 2) were higher in the high-N treatments than in the non-N or low-N treatments. Table 15.1 shows the influence of the different forms of nitrogen treatment on radiocesium activity in the aboveground (experiment 3). The highest activity occurred with ammonium sulfate (approximately 3.7 times the non-N treatment), the next highest activity occurred with ammonium nitrate (approximately 2.4 times the non-N treatment), followed by calcium nitrate (approximately 2.2 times the non-N treatment). The concentrations of radiocesium in the

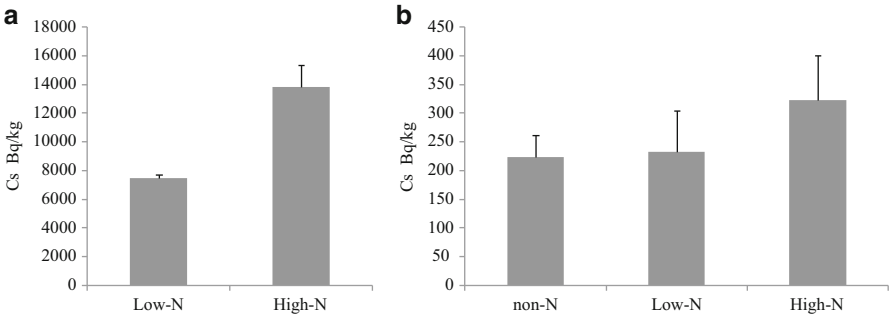

Fig. 15.1 (**a**) Experiment 1. The plants were cultured until maturity within 1 L pot, and the seed was analyzed. (**b**) Experiment 2. The plants were cultureed in Iitate village, Fukushima prefecture, and the aboveground biomass was analyzed

Table 15.1 Radiocesium activities and concentrations of base cations in soybean aboveground biomass after nitrogen fertilization treatments (Experiment 3)

Treatment		Cs	K	Ca	Na	P	Dry weight	Height
		Bq kg^{-1}	mg g^{-1}	mg g^{-1}	mg g^{-1}	mg g^{-1}	g $plant^{-1}$	cm
(Control)	Non-N	440	21	3.3	0.09	2.0	1.6	28
Calcium nitrate	Low-N	464	22	4.8**	0.09	2.0	1.6	30
	Hihg-N	984	24	8.1**	0.22*	1.5	1.3	17*
Ammonium nitrate	Low-N	642	22	3.6	0.12	2.6	1.4	25
	Hihg-N	1077**	19	3.4	0.09	2.3	1.6	29
Ammonium sulfate	Low-N	750	21	3.5	0.09	2.0	1.6	30
	Hihg-N	1634**	21	3.1	0.12	2.9	1.5	25

*$p < 0.05$, **$p < 0.01$ compared to the control (Dunnet's test)

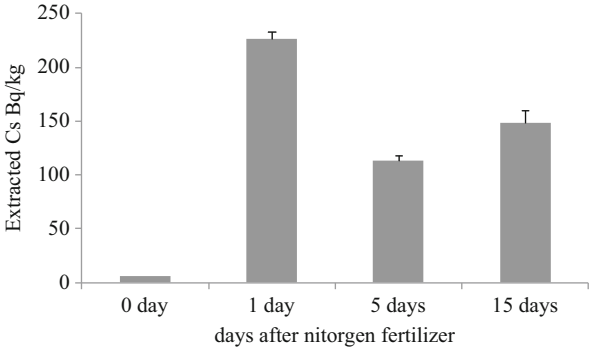

Fig. 15.2 Radiocesium extracted from the soil after nitrogen fertilization (Experiment 4)

aboveground biomass were higher in nitrogen-fertilized plants than in plants without added nitrogen. Figure 15.2 shows the radiocesium activity in soil with applied nitrogen (experiment 4). The amount of extracted radiocesium increased a day after fertilization and remained higher even after 15 days of nitrogen application.

15.4 Discussion

The radiocesium concentration in seed and aboveground biomass increased as the amount of nitrogen fertilizer increased. The different forms of nitrogen treatment increased the radiocesium concentration of soybean in the order ammonium sulfate > ammonium nitrate > calcium nitrate. Hence, ammonium-nitorogen increased radiocesium absorption more than nitrate. Furthermore, the amount of radiocesium extracted from the soil, which is considered potentially available for plant absorption, was increased by ammonium-nitrogen fertilization.

Geometrically adapted cesium ions are fixed to the clay mineral, and the radiocesium adsorbed to the soil particles was probably not available for plant uptake. But the ionic radius of the ammonium ion is similar to that for the cesium

ion [10], ammonium exchanged, and released radiocesium from the soil. We found that the amount of radiocesium extracted by ammonium fertilizer increased the day after fertilization; therefore, soybean could absorb radiocesium. In addition, the ammonium and cesium ions are both univalent cations, and ammonium has been found to restrict cesium absorption in the hydroponics [9–11]. This study was used by soil. It was considered that ammonium oxidizes to nitrate during cultivation, and ammonium fertilization did not restrict the radiocesium absorption of soybean. Moreover, we considered that potassium absorption might compete with ammonium absorption because both ions are univalent cations; hence, the soybeans may lack potassium. A lack of potassium has been found to increase cesium absorption [9, 12, 13]. However, the potassium concentrations in soybean did not decrease with ammonium fertilization. Therefore, we suggest that the increased activity of radiocesium in soybean due to ammonium fertilization was not because of a lack of potassium.

Soybean cultivation typically follows rice cultivation. To assist the recovery and revitalization of agricultural industries in Fukushima Prefecture, we suggest that special care is required to select the appropriate kind of fertilizer and to start cultivating soybean on fields that have higher available nitrogen than the regular cultivated fields. It is important to clarify the mechanism of cesium availability in response to nitrogen fertilizers to cope with cesium contamination in crops.

References

1. Yasunari TJ, Stohl A, Hayano RS, Burkhart JF, Eckhardt S, Yasunari T (2011) Cesium-137 deposition and contamination of Japanese soils due to the Fukushima nuclear accident. Proc Natl Acad Sci U S A 108:19530
2. Zheng J, Tagami K, Bu W, Uchida S, Watanabe Y, Kubota Y, Fuma S, Ihara S (2014) $^{135}Cs/^{137}Cs$ isotopic ratio as a new tracer of radiocesium released from the Fukushima nuclear accident. Environ Sci Technol 48:5433
3. Nihei N (2013) Radioactivity in agricultural products in Fukushima. In: Nakanishi TM, Tanoi K (eds) Agricultural implications of the Fukushima nuclear accident. Springer, Tokyo/New York, pp 73–85
4. Hamada N, Ogino H, Fujimichi Y (2012) Safety regulations of food and water implemented in the first year following the Fukushima nuclear accident. Radiat Res 53:641
5. Fukushima Prefecture (2011) (Toward a new future of Fukushima): http://www.new-fukushima.jp/monitoring/en/ Accessed 10 May 2015
6. Nihei N (2015) Monitoring inspection in Fukushima prefecture and radiocesium absorption of soybean (in Japanese). Isot News 73:118–123
7. Nihei N, Tanoi K, Nakanishi TM (2015) Inspections of radiocesium concentration levels in rice from Fukushima Prefecture after the Fukushima Dai-ichi Nuclear Power Plant accident. Scientific reports 5, Article number: 8653–8658(2015/3)

8. Zhu YG, Shaw G, Nisbet AF, Wilkins BT (2000) Effects of external potassium supply on compartmentation and flux characteristics of radiocaesium in intact spring wheat roots. Ann Bot 85:293–298
9. Sanchez AL, Wright SM, Smolders E, Nayor C, Stevens PA, Kennedy VH, Dodd BA, Singleton DL, Barnett CL (1999) High plant uptake of radiocesium from organic soils due to Cs mobility and low soil K content. Environ Sci Technol 33:2752–2757
10. Tensyo K, Yeh KL, Mitsui S (1961) The uptake of strontium and cesium by plants from soil with special reference to the unusual cesium uptake by lowland rice and its mechanism. Soil Plant Food 6:176
11. Ohmori Y et al (2014) Difference in cesium accumulation among rice cultivars grown in the paddy field in Fukushima Prefecture in 2011 and 2012. J Plant Res 127:57–63
12. Cline JF, Hungate FP (1960) Accumulation of potassium, cesium137, and rubidium86 in bean plants grown in nutrient solutions. Plant Physiol 35:826. doi:10.1104/pp.35.6.826
13. Evans EJ, Dekker AJ (1969) Effect of nitrogen on cesium 137 in soils and its uptake by oat plants. Can J Soil Sci 49:349–355

Chapter 16
Concentrations of $^{134, 137}$Cs and ^{90}Sr in Agricultural Products Collected in Fukushima Prefecture

Hirofumi Tsukada, Tomoyuki Takahashi, Satoshi Fukutani, Kenji Ohse, Kyo Kitayama, and Makoto Akashi

Abstract On April 1, 2012, new Standard Limits for radionuclide concentrations in food were promulgated, superseding the Provisional Regulation Values in Japan set in 2011. The new Standard Limits are calculated based on 1 mSv y^{-1} of annual internal radiation dose through food ingestion of ^{134}Cs, ^{137}Cs, ^{90}Sr, Pu and ^{106}Ru, which were detected or possibly released into the environment from the accident at the TEPCO Fukushima Daiichi Nuclear Power Stations (FDNPS). The concentrations of the radionuclides were based on the values of radiocesium ($^{134, 137}$Cs) and of the other radionuclides (^{90}Sr, Pu and ^{106}Ru); the ratio observed in the determination or predicted concentrations in the soils from the FDNPS accident was used for estimating the concentration of the other radionuclides by means of the ratio against ^{137}Cs. The new Standard Limit of radiocesium in general foods was defined to be 100 Bq kg^{-1} fresh weight by the Ministry of Health, Labour and Welfare. In the present study the concentration of radiocesium was measured in agricultural products collected mostly in Fukushima-shi and Date-shi, Fukushima Prefecture, in 2012 and 2013. The average concentration of radiocesium in agricultural plants in 2012 was 7.6 (<0.2–40) Bq kg^{-1} fresh weight, decreasing to 2.0 (<0.1–14) Bq kg^{-1} fresh weight in 2013, which was approximately one-fourth of the concentration in 2012. The concentration of ^{90}Sr in agricultural products

H. Tsukada (✉)
Institute of Environmental Radioactivity, Fukushima University, 1 Kanayagawa, Fukushima-shi, Fukushima 960-1296, Japan
e-mail: hirot@ipc.fukushima-u.ac.jp

T. Takahashi • S. Fukutani
Research Reactor Institute, Kyoto University, 2 Asashiro-Nishi, Kumatori-cho, Sennan-gun, Osaka 590-0494, Japan

K. Ohse • K. Kitayama
Fukushima Future Center for Regional Revitalization, Fukushima University, 1 Kanayagawa, Fukushima-shi, Fukushima 960-1296, Japan

M. Akashi
National Institute of Radiological Sciences, 4-9-1 Anagawa, Inage-ku, Chiba-shi, Chiba 263-8555, Japan

T. Takahashi (ed.), *Radiological Issues for Fukushima's Revitalized Future*,
DOI 10.1007/978-4-431-55848-4_16

collected in Fukushima Prefecture in 2013 was 0.0047–0.31 Bq kg^{-1} fresh weight, which was a similar range to those collected throughout Japan. The concentration ratio of $^{90}Sr/^{137}Cs$ in the agricultural plants collected from the area 5 km west from the Nuclear Power Stations (difficult-to-return zone) was lower than the predicted $^{90}Sr/^{137}Cs$ ratio, which was calculated using the ratio in the soils and soil-to-plant transfer factors.

Keywords Agricultural product • New standard limits • $^{134, 137}Cs$ • ^{90}Sr • $^{90}Sr/^{137}Cs$ ratio

16.1 Introduction

Significant quantities of radionuclides were released into the environment from the TEPCO's Fukushima Daiichi Nuclear Power Stations (FDNPS) accident in March 2011. Radiocesium ($^{134, 137}Cs$) is the major radionuclide released by the accident and an important radionuclide for the assessment of radiation exposure to the public. Other relatively long half-life radionuclides such as ^{90}Sr, Pu, etc. are also important radionuclides for radiation dose estimation through long-term food ingestion. The new Standard Limits for radionuclides in foods was established by the Ministry of Health, Labour and Welfare on April 1, 2012. The limits were determined on the basis of 1 mSv y^{-1}. The limit in general foods is 100 Bq kg^{-1} of radiocesium, including the contribution of ^{90}Sr, Pu and ^{106}Ru, determined by using the actual concentration in the soils from the accident (estimated data for ^{106}Ru) and soil-to-transfer factor. However, the public has been concerned about food contamination, especially ^{90}Sr. In the present study the concentrations of radiocesium and ^{90}Sr in agricultural and animal products produced in Fukushima Prefecture were determined, and compared with the values of the new allowable Standard Limits.

16.2 Materials and Methods

Agricultural and animal products, limited to those produced within the Fukushima Prefecture, were collected from markets located mostly in Fukushima-shi and Date-shi. Table 16.1 contains a list of 120–5000 g samples of 11 spices in 2012 (40 samples) and 2013 (42 samples). The agricultural plants were washed, peeled, and then the edible parts were cut into small pieces. Each sample was dried at 70 °C for 1 week and pulverized in a stainless steel cutter blender before being analyzed for radiocesium. The animal samples were also cut into small pieces. The samples were compressed into a plastic container (47 mm in diameter and 50 mm in height) and the concentration of radiocesium and ^{40}K determined with a Ge detector connected to a multichannel analyzer system by counting for 9400–33,000 s. The

Table 16.1 Collected agricultural and animal products in Fukushima Prefecture in 2012 and 2013

Agricultural and animal products	Collected sample
Rice	Brown rice
Potatoes	Potato, Sweet potato, Eddoe
Savory herbs	Japanese ginger
Leaf and stem vegetables	Komatsuna, Malabar spinach, String bean, Cabbage, Welsh onion, Leek, Spinach, Japanese honeywort, Turnip (leaf and stem), Turnip rape, Mugwort, Asparagus, Onion
Root vegetables	Turnip, Burdock, Radish, Carrot
Pulses	Green soybean, Green bean, Cowpea, Black soybean
Fruity vegetables	Cucumber, Tomato, Green pepper, Eggplant, Pumpkin, Small green pepper, Okra, Broccoli, Snap garden pea, Zucchini, Wax gourd
Fruits	Pear, Apple, Persimmon, Huckleberry, Plum, Peach, Blue berry, Japanese plum
Wild vegetables	Udo, Butterbur, Momijigasa
Other agricultural plants	Jew's-ear mushroom, Shiitake mushroom, Hen-of-the-woods mushroom, Edible chrysanthemum, Japanese pepper (leaf)
Animal products	Chicken, pork, egg

detection efficiency of the Ge detector was dependent on the sample thickness and was obtained using the mixed standard radionuclides material made by the Japan Radioisotope Association. Counting statistics standard deviations for ^{137}Cs concentration in the sample were less than 10 % of the value.

Soil and agricultural samples were collected from 10 agricultural fields located both outside and within the more than 50 mSv y^{-1} of the external radiation dose zone (difficult-to-return zone, Okuma) in Fukushima Prefecture in 2013 and 2014 (Fig. 16.1) . Shiitake mushroom and its mushroom bed for cultivation was also collected. A stainless steel core sampler was used to collect soil cores 5 cm in diameter and 20 cm in depth at 5 points evenly distributed in each field. Twenty kilogram of each agricultural sample was collected from each field. The soil core samples collected from each field were dried at 50 °C for 1 week and then passed through a 2 mm sieve. The soil samples in each field were thoroughly mixed. The agricultural samples were washed, peeled, and then the edible parts were cut into small pieces. Approximately 100 g of dried sample was pulverized in a stainless steel cutter blender before being analyzed for radiocesium. The rest of the dried agricultural samples were washed at a temperature below 450 °C for analysis of ^{90}Sr. The dried soil and agricultural samples were compressed into plastic containers and the concentrations of radiocesium and ^{40}K determined. A radioanalytical method for ^{90}Sr was performed according to the previously reported method [1]. The ash plant samples (20–50 g) were decomposed with HNO_3, H_2O_2 and HCl after the addition of the Sr carrier. The soil samples (100 g) were heated at 450 °C and then extracted with 12 M HCl after the addition of the Sr carrier. The solution was filtered and the residue discarded. The solution was adjusted to >pH 10 with

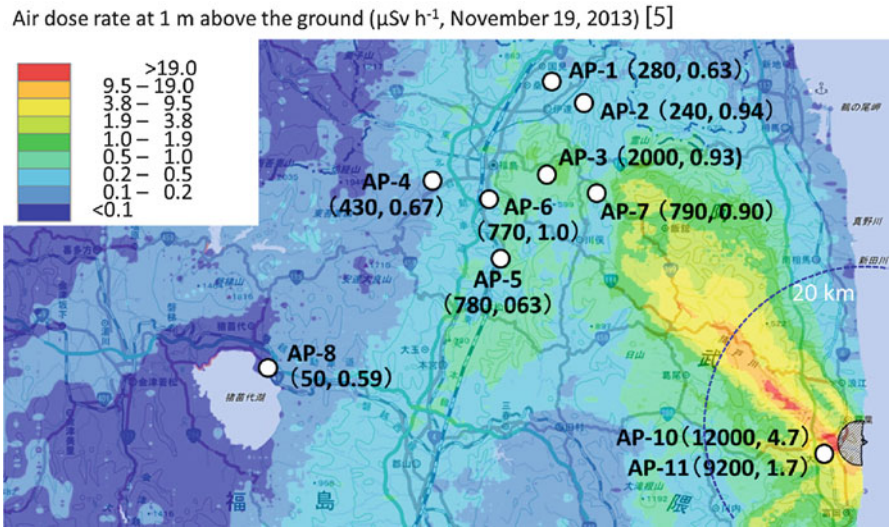

Fig. 16.1 Concentrations of ^{137}Cs and ^{90}Sr (Bq kg^{-1} dry weight) in cultivated soil ($n = 10$) collected from Fukushima Prefecture in 2014. Point numbers show the sampling agricultural plants indicated in Table 16.3 and the values in parentheses are the concentrations of ^{137}Cs (former) and ^{90}Sr (latter) in cultivated soil

NaOH and then $SrCO_3$ precipitated by adding Na_2CO_3. The $SrCO_3$ precipitate was dissolved in HCl and then the oxalates re-precipitated at pH 4.2 by adding oxalic acid. The supernatant was decanted and the oxalate precipitation dissolved in HNO_3. Strontium in the solution was separated from Ca by the cation ion-exchange method, and then the filtrated precipitate was dissolved with water. Any radioactive impurity was eliminated by scavenging on $BaCrO_4$ and $Fe(OH)_3$. An ammonium carbonate solution was added to the solution after scavenging, and the $SrCO_3$ precipitate was filtered using a cellulose filter paper. The recovery of Sr was estimated by measuring the stable Sr with ICP-AES and then a disk sample prepared for beta-counting for 6000–60,000 s.

16.3 Results and Discussion

The concentrations of radiocesium in agricultural products collected in Fukushima Prefecture in 2012 and 2013 are listed in Table 16.2. The average concentration of radiocesium collected in 2013 was 2.0 ± 2.7 (<0.046–14) Bq kg^{-1} fresh weight, which was one-fourth of that in 2012 (7.6 ± 10, <0.11–40 Bq kg^{-1} fresh weight), and the concentrations of radiocesium in all the samples were less than the new Standard Limits. The concentrations of radiocesium in agricultural products decrease with time elapsed, and the reasons are as follows:

Table 16.2 Concentration ranges of ^{134}Cs, ^{137}Cs and ^{40}K in agricultural and animal products (grouping noted in Table 16.1) collected from Fukushima Prefecture in 2012 and 2013

Agricultural and animal products	2012				2013			
	^{134}Cs	^{137}Cs	^{40}K	n	^{134}Cs	^{137}Cs	^{40}K	n
	Concentration (Bq kg^{-1} fresh weight)				Concentration (Bq kg^{-1} fresh weight)			
Rice	1.0–2.5	1.4–4.9	34–55	3	<0.58	0.66	82	1
Potatoes	0.25–2.8	0.53–4.4	120–190	3	0.42–1.6	0.86–3.5	110–160	3
Savory herbs				–	1.2	2.4	130	1
Leaf and stem vegetables	0.08–2.0	0.17–3.8	39–140	8	<0.11–2.8	<0.11–4.7	42–280	15
Root vegetables				–	<0.022–0.41	<0.024–0.83	78–140	5
Pulses	5.9–15	10–25	160–560	3	1.1	2.2	210	1
Fruity vegetables	<0.063–2.3	<0.052–3.6	48–180	8	<0.046–0.85	<0.10–2.1	53–180	9
Fruits	0.16–13	0.25–23	26–170	7	0.77–0.92	1.6–2.1	45–47	2
Wild vegetables					0.26–4.4	0.51–9.6	94–160	4
Other agricultural plants	1.4–5.4	2.4–8.8	18–100	4	1.1	2.1	110	1
Animal products	<0.85	<0.68	60–110	4				–

1. Decay of radiocesium activities, especially ^{134}Cs (half-life, 2.1 y)
2. Countermeasure with the application of K fertilizer for reducing uptake of radiocesium in plants
3. Aging effect in soil, which radiocesium in exchangeable fraction decreases and that in strongly bound fraction increases with time elapsed [2, 3]
4. Decreasing radiocesium contents in soil by erosion, etc.

The concentration of radiocesium in agricultural plants drastically decreases immediately after the accident, and the rate of the decrease of radiocesium concentration in plants has gradually slowed as more time has lapsed. The reported mean concentration of radiocesium in a duplicate diet collected from Fukushima Prefecture in December 2011 was 1.5 Bq kg^{-1} [4], which was lower than that in 2013 as determined in this study. This is because the concentration of radiocesium in foods determined by a duplicate method decreased during processing and cooking and market dilution effect.

The concentrations of $^{134, 137}$Cs and ^{90}Sr were determined in surface soils and agricultural plants collected from both outside and within the difficult-to-return zone in Fukushima Prefecture. The concentration of radiocesium in the agricultural soils outside the zone is decreasing because of plowing, migration, erosion, etc. However, the soil within the difficult-to-return zone (experimental field 5 km west from the

Table 16.3 Concentrations of ^{134}Cs, ^{137}Cs, ^{40}K and ^{90}Sr in agricultural plants collected from Fukushima Prefecture in 2012 and 2013

Sample no.	Agricultural plant	Dry matter content	Concentration			
			^{134}Cs	^{137}Cs	^{40}K	^{90}Sr
		(%)	(Bq kg^{-1} fresh weight)			
AP-1	Komatsuna	4.5	0.030 ± 0.0036	0.055 ± 0.0044	100 ± 0.34	0.054 ± 0.0027
AP-2	Cucumber	4.2	0.063 ± 0.0074	0.11 ± 0.008	66 ± 0.57	0.013 ± 0.0011
AP-3	Brown rice	89	0.74 ± 0.054	1.6 ± 0.077	65 ± 1.9	0.013 ± 0.0018
AP-4	Potato	19	1.7 ± 0.026	3.9 ± 0.039	130 ± 0.88	0.012 ± 0.00093
AP-5	Carrot	9.1	0.36 ± 0.032	0.78 ± 0.040	130 ± 1.7	0.031 ± 0.0022
AP-6	Soy bean	90	3.7 ± 0.32	8.8 ± 0.47	540 ± 14	0.30 ± 0.014
AP-7	Persimmon	14	1.5 ± 0.047	3.6 ± 0.074	56 ± 1.2	0.0086 ± 0.00050
AP-8	Edible chrysanthemum (flowers)	8.8	0.072 ± 0.0040	0.17 ± 0.0059	86 ± 0.32	0.044 ± 0.0039
AP-9	Shiitake mushroom	11	2.2 ± 0.093	5.1 ± 0.14	85 ± 2.3	0.0047 ± 0.00032
AP-10[a]	Pumpkin	15	27 ± 0.79	80 ± 1.3	75 ± 5.9	0.31 ± 0.0061
AP-11[a]	Cabbage	5.8	17 ± 0.38	50 ± 0.68	64 ± 3.5	0.21 ± 0.0057
	Various agricultural plants[b]		ND[c] ~ 4.9	ND ~ 10		ND ~ 0.91

The errors indicate one standard deviation of counting statistics
[a]Collected from the difficult-to-return zone (Okuma)
[b]Samples collected throughout Japan excluding Fukushima Prefecture in 2013 (data from Environmental Radioactivity and Radiation in Japan [6])
[c]Not detected

Nuclear Power Stations in Okuma) is still highly contaminated with radiocesium (Fig. 16.1). The concentration of ^{90}Sr in the soils collected outside the zone is low with no differences among the values. In contrast, ^{90}Sr concentration in the soils collected within the zone was several times higher than that outside the zone. However, the concentration of ^{90}Sr in the soils collected both outside and within the zone is within the range collected throughout Japan except Fukushima (ND-5.9 Bq kg^{-1}, data from Environmental Radioactivity and Radiation in Japan [6]). The concentration of radiocesium in the plants collected outside of the difficult-to-return zone (Table 16.3) is similar to the range shown in Table 16.2. The concentration of radiocesium in the agricultural plants within the zone was still higher than that outside the zone (Table 16.3); however, part of the plants cultivated

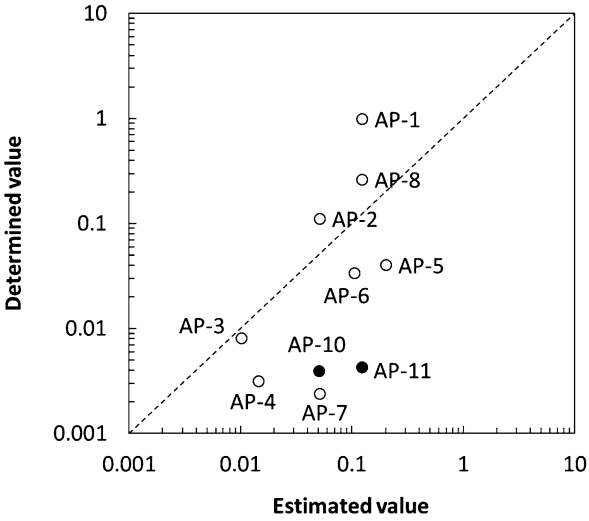

Fig. 16.2 Comparison of ^{90}Sr/^{137}Cs concentration ratio between the estimated value and the determined value in agricultural plants. *Plotted numbers* indicate sample no. in Table 16.2. The *solid-black circles* (AP-10 and AP-11) were collected within the difficult-to-return zone

in the experimental field was lower than the new Standard Limits [7]. The range of ^{90}Sr concentration in the plants collected outside the zone is 0.0047–0.30 Bq kg^{-1} fresh weight, and those collected within the zone were 0.31 (pumpkin) and 0.21 (cabbage). These data are also within the range collected throughout Japan except Fukushima (ND-0.91 Bq kg^{-1} fresh weight, data from Environmental Radioactivity and Radiation in Japan [6]).

The new Standard Limits of radiocesium include the contribution of ^{90}Sr concentration in general foods. The concentration ratio of ^{90}Sr/^{137}Cs in the foods was predicted by using observed ^{90}Sr/^{137}Cs concentration ratio (0.003) [8] in the soils from the FDNPS accident and the reported soil-to-plant transfer factor [9, 10], and the concentration of ^{90}Sr in foods was determined by multiplying the predicted ^{90}Sr/^{137}Cs ratio in foods by the measured ^{137}Cs value in foods. Therefore, the propriety between the predicted and the measured ^{90}Sr/^{137}Cs ratio in foods (Fig. 16.2) needs to be evaluated. The measured concentration ratio of ^{90}Sr/^{137}Cs in the plants, except for three samples (AP-1, komatsuna; AP-2, cucumber; AP-8, edible chrysanthemum), was lower than the predicted ^{90}Sr/^{137}Cs ratio, and the determined ratio in the two samples collected within the difficult-to-return zone (Okuma), which may have a large contribution from the accident, was also lower than the predicted ^{90}Sr/^{137}Cs ratio. The concentration of ^{90}Sr in the soils collected from the three fields, where the ^{90}Sr/^{137}Cs concentration ratio in the plants overestimated the predicted ratio, was similar in range to the global fallout deposited in the soil. Therefore it is necessary to attribute the ^{90}Sr contents in the plants as being derived from the global fallout from several decades ago.

Internal radiation doses from radiocesium through food ingestion for adult males and females (over the age of 19) were estimated. Measured and predicted data for the radiocesium concentration in food categories were used. The concentration of ^{137}Cs in the animal products including milk collected in 2012 and 2013 was not

detected, and the average value of the detection limits (0.6 Bq kg^{-1}) in the animal products was used for the dose estimation. Drinking water pathway was not included for the dose estimation because it was lower than the detection limit. The estimated internal radiation doses through food ingestion for males and females were 0.066 and 0.052 mSv y^{-1} in 2012, and those in 2013 were 0.016 and 0.012, respectively, reflecting the decreases in the concentration of radiocesium in foods with time elapsed. It was also reported that the internal radiation dose from radiocesium in Fukushima Prefecture in 2012 was 0.0039–0.0066 mSv y^{-1} by the market basket method [11], which was one order of magnitude lower than that in this study. This is attributed to the fact that the collected foods by the market basket method usually included products both within and outside of Fukushima Prefecture, and the concentration of radiocesium in the foods decreased by market dilution. On the other hand, the samples collected in this study were produced only in Fukushima Prefecture and were not influenced by the market dilution effect. The internal radiation doses from radiocesium by the duplicate diet method in Fukushima Prefecture were reported as 0.026 mSv y^{-1} in 2011 [4] and 0.0022 mSv y^{-1} in 2012 [11]. The internal radiation dose from radiocesium through food ingestion determined by the duplicate diet method is lower than that by the market basket method because of processing and cooking, and it is assumed that those values decrease with time elapsed.

Acknowledgement This work was supported by MHLW KAKENHI Grant. We are grateful to Messrs. A. Sato (Ichii Co. Ltd.) and M. Kanno (Citizens for Revitalization of Oguni after Nuclear Disaster) for sample collection, and Dr. P. T. Lattimore for his useful suggestion and comments. We thank Mr. A. Kanno, Mses. C. Suzuki, W. Horiuchi and M. Kato for sample pretreatment.

References

1. Tsukada H, Takeda A, Takahashi T, Hasegawa H, Hisamatsu S, Inaba J (2005) Uptake and distribution of ^{90}Sr and stable Sr in rice plants. J Environ Radioact 81:221–231
2. Takeda A, Tsukada H, Nakao A, Takaku Y, Hisamatsu S (2013) Time-dependent changes of phytoavailability of Cs added to allophanic Andosols in laboratory cultivations and extraction tests. J Environ Radioact 122:29–36
3. Tsukada H (2014) Behavior of radioactive cesium in soil with aging. Jpn J Soil Sci Plant Nutr 85:77–79 (in Japanese)
4. Harada KH, Fujii Y, Adachi A, Tsukidate A, Asai F, Koizumi A (2013) Dietary intake of radiocesium in adult residents in Fukushima Prefecture and neighboring regions after the Fukushima nuclear power plant accident: 24-h food-duplicate survey in December 2011. Environ Sci Tech 47:2520–2526
5. Nuclear Regulation Authority. Monitoring information of environmental radioactivity level. http://ramap.jmc.or.jp/map/eng/

6. Environmental Radioactivity and Radiation in Japan. http://www.kankyo-hoshano.go.jp/en/index.html
7. Ohse K, Kitayama K, Suenaga S, Matsumoto K, Kanno A, Suzuki C, Kawatsu K, Tsukada H (2014) Concentration of radiocesium in rice, vegetables, and fruits cultivated in evacuation area in Okuma Town, Fukushima. J Radioanal Nucl Chem 303:1533–1537
8. Ministry of Health, Labour and Welfare. http://www.mhlw.go.jp/stf/shingi/2r98520000023nbs-att/2r98520000023ng2.pdf
9. IAEA (2010) Handbook of parameter values for the prediction of radionuclide transfer in terrestrial and freshwater environment, vol 472, Technical report series. International Atomic Energy Agency, Vienna
10. Tsukada H, Nakamura Y (1998) Transfer factors of 31 elements in several agricultural plants collected from 150 farm fields in Aomori, Japan. J Radioanal Nucl Chem 236:123–131
11. Ministry of Health, Labour and Welfare. http://www.mhlw.go.jp/shinsai_jouhou/shokuhin.html

Chapter 17
Analysis of Factors Causing High Radiocesium Concentrations in Brown Rice Grown in Minamisoma City

Takashi Saito, Kazuhira Takahashi, Toshifumi Murakami, and Takuro Shinano

Abstract Despite a concentration of exchangeable K of >208 mg kg^{-1} dry weight in soil, the brown rice grown in Minamisoma City in 2013 had a higher concentration of radiocesium than the new Japanese standard (100 Bq kg^{-1}) for food. To analyze the factors affecting the radiocesium concentration in brown rice, we carried out pot tests using paddy soil and irrigation water collected in Minamisoma City. Rice seedlings were planted in 5-L pots containing Minamisoma soil, in which the exchangeable K was 125 mg kg^{-1} dry weight, and were irrigated with tap water or irrigation water collected in Minamisoma City. There was no difference in the Cs-137 concentration in brown rice between the two types of irrigation. Then we grew rice in the Minamisoma soil and two soils collected in Nakadori, Fukushima Prefecture. Cs-137 uptake in the Minamisoma soil was intermediate between the uptake rates in the Nakadori soils, showing that the Minamisoma soil was not special in radiocesium uptake. Finally, we grew rice in soil without radiocesium near the Fukushima Daiichi Nuclear Power Plant in 2014. Although the maximum value of Cs-137 in brown rice was 18 Bq kg^{-1}, below the standard, radiocesium was attached to the surface of the foliage.

Keywords Cs-137 • Brown rice • Exchangeable K • Irrigation water • Minamisoma City

T. Saito (✉) • K. Takahashi
Agro-environment Division, Fukushima Agricultural Technology Centre, 116 Shimonakamichi, Takakura-aza, Hiwada-machi, Koriyama, Fukushima 963-0531, Japan
e-mail: saito_takashi_01@pref.fukushima.lg.jp

T. Murakami • T. Shinano
NARO Tohoku Agricultural Research Centre, 50 Harajukuminami, Arai Fukushima, Fukushima 960-2156, Japan

T. Takahashi (ed.), *Radiological Issues for Fukushima's Revitalized Future*,
DOI 10.1007/978-4-431-55848-4_17

17.1 Introduction

Following the accident at the Fukushima Daiichi Nuclear Power Plant on 11 March 2011, soils became contaminated with radiocesium (Cs-134 and Cs-137). To reduce the uptake of radiocesium by rice, growers have been adding potassium (K) fertilizer to their paddy fields, as the uptake of Cs decreases with increasing K concentration ([K]) in the soil [1] and the concentration of radiocesium in brown rice decreases at increasing concentrations of exchangeable K in the soil and K^+ in the soil solution [2]. K fertilization offers an effective and practical way to reduce radiocesium uptake by rice from several soil types [3]. Following the accident, the Food Sanitation Law of 2012 reduced the standard for the concentration of radiocesium in food to 100 Bq kg^{-1}. A concentration of >208 mg kg^{-1} dry weight of exchangeable K in soil is recommended for keeping the radiocesium content in brown rice below the standard [4].

However, despite a concentration of exchangeable K of >208 mg kg^{-1} in soil, the brown rice grown in Minamisoma City in 2013 exceeded the new standard [5].

One possible source is irrigation water. Dissolved radiocesium moves more easily into plants from water than from soil [6]. The concentration of dissolved radiocesium in irrigation water drawn from the Ota River in Minamisoma City was higher than that in other parts of Fukushima Prefecture [7].

One possible source is soil. Although Tsumura et al. [8] reported the relationship between the concentration of exchangeable K in soils and Cs-137 uptake in brown rice, however, discussion on radiocesium uptake in brown rice has not been done in same levels of exchangeable K in soil.

Another possible source is dust. The Cs-137 concentration ([Cs-137]) in dust collected in Futaba Town on 19 August 2013 was clearly higher than that at other times [9].

To identify the cause of the high radiocesium concentration in brown rice grown in Minamisoma City, we conducted pot experiments comparing sources of irrigation water and soil types. In addition, we determined the [Cs-137] of rice grown near the nuclear plant.

17.2 Materials and Methods

17.2.1 Irrigation Water

We collected 20 L of water on six dates (shown in Fig. 17.1) from the Ota River and passed it through 0.45-μm filters. Suspended matter collected on the filters was compressed into cylindrical polystyrene containers (i.d. 5.0 cm, o.d. 5.6 cm, height 6.8 cm) for analysis. The filtrates were concentrated to 2 L by heat and then placed in 2-L Marinelli beakers for analysis as described below. The concentrations of dissolved Cs-137 were 0.15–0.42 Bq L^{-1}, and those of suspended Cs-137 were 0.09–0.17 Bq L^{-1} (Fig. 17.1). [Cs-137] in tap water was 0.02 Bq L^{-1}.

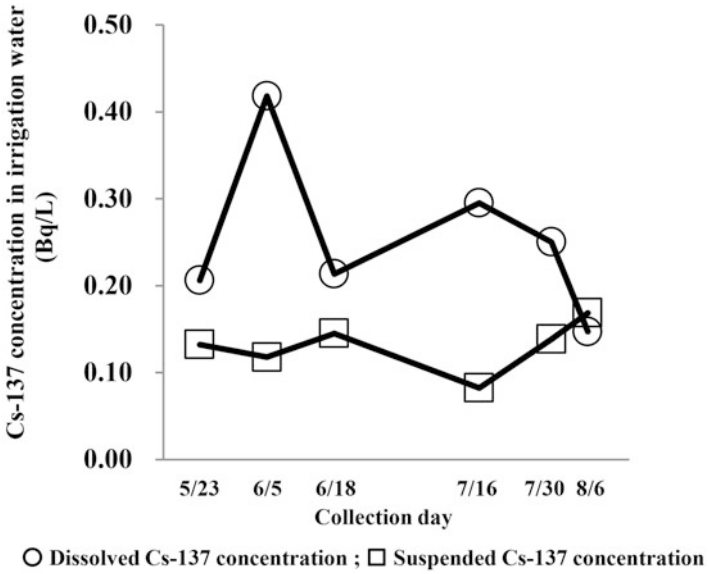

Fig. 17.1 [Cs-137] in irrigation water used for pot experiments. Error bars represent standard errors ($n = 3$). $^*P < 0.05$ (Student's t-test) between tap water and irrigation water

Table 17.1 Chemical properties of soils used for pot experiment

Name	Soil types	pH(H_2O)	Total C (g kg^{-1})	K (mg kg^{-1})	Exchangeable Ca (mg kg^{-1})	Mg (mg kg^{-1})	CEC (cmolc kg^{-1})
Minamisoma	Gray lowland soil	6.3	14	150	1640	390	9.1
Soil A	Andosol	5.6	79	25	1220	170	15.2
Soil B	Gray lowland soil	6.6	9.1	134	2160	553	11.4

17.2.2 Soils

Soils were collected from the field in April 2014. Experiment 1 used a contaminated Glay lowland soil collected from the top 15 cm of a paddy field in Minamisoma City where the concentration of radiocesium in brown rice grown in 2013 exceeded 100 Bq kg^{-1}.

Experiment 2 used three soils (Table 17.1): the Minamisoma Gray lowland soil; an Andosol collected from 0 to 15 and 15–30 cm depth in a paddy field in northern Fukushima Prefecture where the concentration of radiocesium in brown rice grown in 2011 exceeded 500 Bq kg^{-1} (soil A); and a Gray lowland soil collected from 0 to 15 and 15–30 cm depth in a paddy field at the Fukushima Agricultural Technology Centre (FATC), where the concentration of radiocesium in brown rice grown in 2011 was below the limit of quantification (<20 Bq kg^{-1}) (soil B).

Experiment 3 used an uncontaminated Gray lowland soil collected from the subsoil (beneath 15 cm depth) of a paddy field at FATC. The [Cs-137] in the soil was 35 Bq kg^{-1} dry weight.

17.2.3 Pot Experiments

Soils were air dried, thoroughly mixed, and passed through a 2-mm sieve. On 8 May 2014, rice seeds (*Oryza sativa* L. 'Maihime') were sown in granular culture soil. On 6 June, four seedlings were transplanted into each 5-L Wagner pot (diam. 16 cm, height 25 cm), which held 3.0 kg dry weight of soil. Each pot also received a basal dressing of 1.0 g of ammonium sulfate and calcium superphosphate and mixed into the soil. The water level was kept at a depth of 3–5 cm during the experiments. All experiments were conducted at FATC (and experiment 3 at Okuma Town also) under natural light. All treatments had three replicates. The rice plants were harvested on 9 October 2014, and samples of brown rice and leaves were oven dried at 40 °C for 24 h.

17.2.3.1 Experiment 1

The [Cs-137] in the contaminated Minamisoma soil was 1500 Bq kg^{-1} dry weight. No KCl was applied. Pots were watered with either tap water or irrigation water. Each pot received a total of 11–16 L during the experiment.

17.2.3.2 Experiment 2

The [Cs-137] in the contaminated Minamisoma soil was adjusted to 1500 Bq kg^{-1} as above. The [Cs-137] in soils A and B was adjusted to 1500 Bq kg^{-1} by mixing the topsoil and subsoil. The exchangeable K content of each was adjusted to 125 or 250 mg kg^{-1} with KCl. Pots were watered with irrigation water used in Experiment 1.

17.2.3.3 Experiment 3

The exchangeable K content of the uncontaminated soil was adjusted to 208 mg kg^{-1} with KCl. All plants were watered with tap water. Treatment pots were moved from the FATC to Okuma Town on 9 July and back to the FATC on 20 August. Control pots remained at the FATC. The pots were protected with a multi-film so that only the leaves were exposed to fallout. Radiocesium contaminations of rice foliage were analyzed by a gamma-ray spectrometry and autoradiography visually. In the autoradiogram analysis, powdered shoot (3 g) was put into a small polyethylene bag (10×7 cm) and the bag was put on the cardboard (40×20 cm, 0.6 mm thickness).

Markers made with potassium chloride (contain 10–26 mg) were attached on the corners of the cardboard samples to obtain a superposition of the autoradiogram and the visible image. An imaging plate (BAS-SR2040 (40 × 20 cm), Fuji-film, Japan) was contacted with the cardboard, and they were put into a paper case together and sandwiched between two lead plates of 4 mm thickness in a dark room. After 7 days exposure the imaging plate was scanned by image scanner (Typhoon FLA 7000, GE Healthcare Bio-Science Co., Ltd., USA) at a spatial resolution of 25 μm. The autoradiography and its visible image were overlapped on image processing software (Photoshop CS4 ver. 11.0, Adobe Co., Ltd., USA).

17.2.4 Soil and Plant Analyses

The chemical properties of the soils were analyzed according to the Editorial Boards of Methods for Soil Environment Analysis [10] (Table 17.1). Soil pH (H_2O) was measured at a soil-to-water ratio of 1:2.5 (w/w). The total carbon content was determined by dry combustion on a Sumigraph NC Analyzer NC-220 F (Sumika Chemical Analysis Service, Ltd., Osaka, Japan). Exchangeable K, calcium, magnesium were determined by the semi-micro Schollenberger method on an atomic absorption spectrophotometer (AA280FS; Varian Technologies Japan Ltd., Tokyo, Japan), and cation exchange capacity is calculated as the sum of these component ions.

The brown rice and leaf samples were compressed into cylindrical polystyrene containers as above, and the [Cs-137] was measured with a Ge gamma-ray detector connected to a multichannel analyzer (GC2020, GC3020, GC3520, GC4020, Canberra USA) for 36,000 s.

17.2.5 Statistical Analyses

Statistical analyses were performed in StatView 5.0 J software (SAS Institute, Berkeley, CA, USA). Analysis of variance (ANOVA) followed by *t*-test or Tukey's multiple comparison test was used to determine the significance of differences in a pairwise comparison matrix.

17.3 Results

17.3.1 Effect of Irrigation Water on Cs-137 Uptake in Rice

In both watering treatments (irrigation and tap water), the concentration of exchangeable K was 125 mg kg^{-1} before planting and 45 mg kg^{-1} after harvest (data not shown). When watered with irrigation water, [Cs-137] in brown rice and

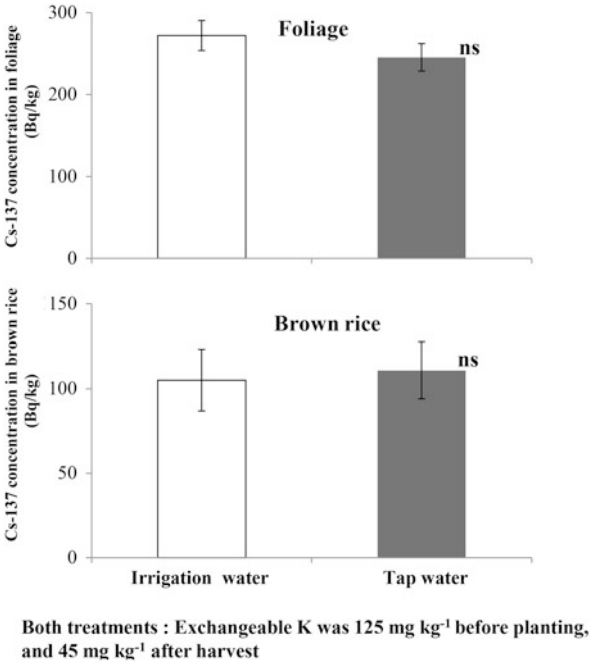

Fig. 17.2 [Cs-137] in foliage and brown rice of plants watered with irrigation or tap water. Error bars represent standard error ($n = 3$). ns, not significantly different; $^*P > 0.05$ (Student's t-test) between irrigation water and tap water

foliage were 105 and 272 Bq kg^{-1} and watered with tap water were 111 and 245 Bq kg^{-1}, respectively (Fig. 17.2). There was no significant difference in the [Cs-137] of brown rice or foliage between treatments.

17.3.2 Effect of Soil Type on Cs-137 Uptake in Rice

When exchangeable K in Minamisoma soil of pot was 34.9 and 52.1 mg kg^{-1} after harvest, the [Cs-137] in the foliage of rice plant grown were 272 and 119 Bq kg^{-1}, respectively (Fig. 17.3). On the other hand, when exchangeable K in soil A of pot was 15.6 and 46.5 mg kg^{-1}after harvest, the [Cs-137] in the brown rice grown was 594 and 215 Bq kg^{-1}, respectively, and higher than that of Minamisoma soil. When exchangeable K in soil B of pot was 56.4 and 78.8 mg kg^{-1}, the [Cs-137] in the brown rice was 30.4 and 12.0 Bq kg^{-1}, respectively, and lower than that of the Minamisoma soil.

When exchangeable K in Minamisoma soil of pot was 34.9 and 52.1 mg kg^{-1} after cultivating, the [Cs-137] in the brown rice grown were 105 and 54.1 Bq kg^{-1}, respectively. On the other hand, when exchangeable K in soil A of pot was 15.6 and 46.5 mg kg^{-1}, the [Cs-137] in the brown rice grown was 206 and93.8 Bq kg^{-1},

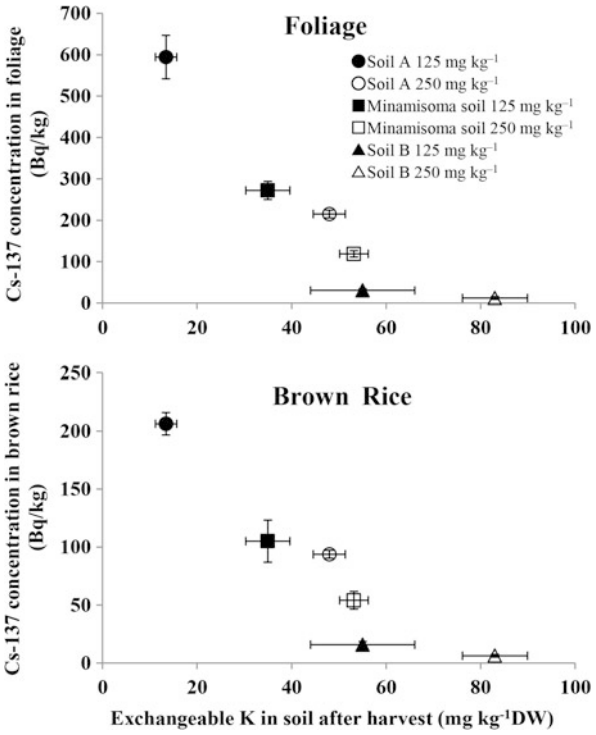

Fig. 17.3 Relationship between [Cs-137] in rice and exchangeable K after harvest in different kind soils or in different K soils. Error bars represent standard errors ($n = 3$)

respectively, and higher than that of the Minamisoma soil. When exchangeable K in soil B of pot was 56.4 and 78.8 mg kg^{-1}, the [Cs-137] in the brown rice was 15.8 and 6.3 Bq kg^{-1}, respectively, and lower than those of Minamisoma soil.

17.3.3 Effect of Site on Acquisition of Cs-137 by Foliage and Brown Rice

There was no significant change in the amount of exchangeable K in either treatment before and after the experiment (data not shown). The [Cs-137] in the brown rice and leaves of plants grown at Okuma Town for 6 weeks was 5–7 times that in the plants kept at the FATC (Fig. 17.4).

Autoradiographs of brown rice and foliage revealed no contamination of either in plants grown at the FATC or in brown rice of plants grown at Okuma Town (Fig. 17.5). However, foliage of plants grown at Okuma Town showed radioactive contamination (Fig. 17.6).

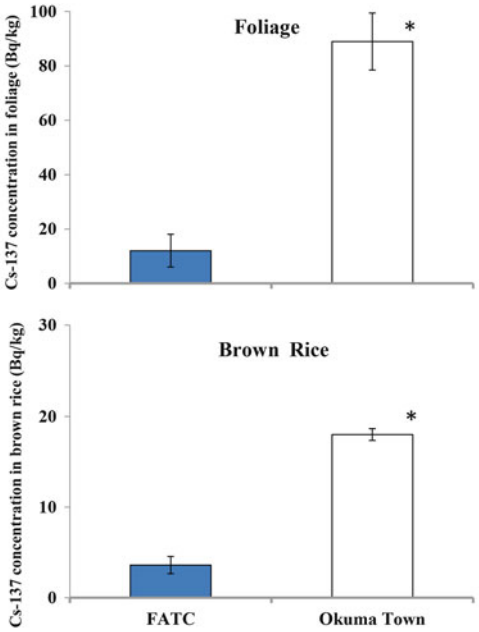

FATC : Exchangeable K was 208 mg kg^{-1} before planting, and 63 mg kg^{-1} after harvest.
Okuma Town: Exchangeable K was 208 mg kg^{-1} before planting, and 67 mg kg^{-1} after harvest.

Fig. 17.4 Translocation of Cs-137 from foliage to brown rice between two sites. Error bars represent standard errors ($n = 3$). *$P < 0.05$ (Student's t-test) between TATC and Okuma Town

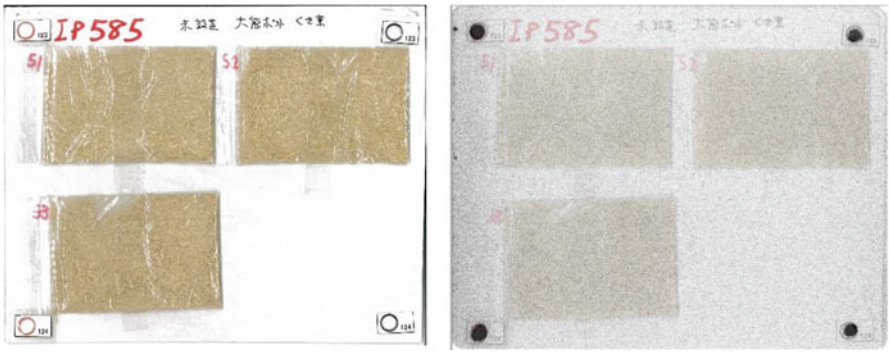

Fig. 17.5 Autoradiographs of foliage rice by FATC

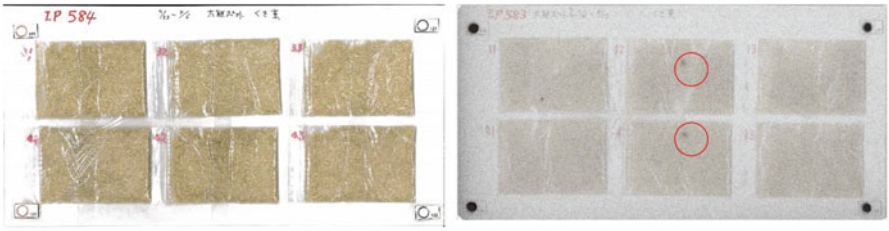

Fig. 17.6 Autoradiographs of foliage rice by Okuma Town

17.4 Discussion

17.4.1 Effect of Irrigation Water on Cs-137 Uptake in Rice

In hydroponic culture with 0.1, 1.0, or 10 Bq L^{-1} Cs-137, the [Cs-137] in brown rice increased with increasing [Cs-137] in the culture solution [6]. However, nutrient uptake can be greater in hydroponic culture than in soil culture because all nutrients are in solution. In contrast, a high level of exchangeable K in soil can limit the transfer of Cs-137 from irrigation water containing low levels of Cs-137 (0.1–1.0 Bq L^{-1}) [11]. We found no significant difference in uptake between water sources; therefore, low levels of exchangeable K in both soils limited Cs-137 uptake by rice plants.

17.4.2 Effect of Soil Type on Cs-137 Uptake in Rice

The Minamisoma soil did not have superior ability to promote Cs-137 uptake (Fig. 17.3). To reduce the [Cs-137] below 100 Bq kg^{-1} would require 40 mg kg^{-1} of exchangeable K in the Minamisoma soil and 50 mg kg^{-1} in soil A. Thus, at a similar level of exchangeable K in the soil, Cs-137 uptake depended on soil type. The high carbon content and low clay content of soil A may have helped to inhibit Cs-137 uptake. Therefore, the Minamisoma soil was not the cause of high [Cs-137] in 2013.

17.4.3 Effect of Site on Acquisition of Cs-137 by Foliage and Brown Rice

The [Cs-137] of rice plants increased greatly during 6 weeks' culture in Okuma Town. Cs-137 derived from the Fukushima accident is still distributed widely around the town. Thus, the rice plants could have taken up more radiocesium from the outside environment.

References

1. Tsukada H, Hasegawa H, Hisamatsu S, Yamasaki S (2002) Transfer of ^{137}Cs and stable Cs from paddy soil to polished rice in Aomori, Tsukuba, Japan. J Environ Radioact 59:351–363
2. Saito T et al (2012) Effect of potassium application on root uptake of radiocesium in rice. In: Proceeding of international system on environmental monitoring and dose estimation of residents after accident of TEPCO's Fukushima Daiichi Nuclear Power Station. Kyoto University Research Reactor Institute Press, Kyoto, pp 165–169
3. Kato (2012) Countermeasures to reduce radiocaesium contamination I paddy rice, soy bean and cabbage. In: International science symposium on combating radionuclide contamination in Agro-soil environment, Fukushima, pp 317–318
4. NARO (2012) http://www.naro.affrc.go.jp/org/tarc/seika/jyouhou/H24/kankyou/H24kankyou012.html (in Japanese, May 2015)
5. MAFF (2014a) http://www.maff.go.jp/j/kanbo/joho/saigai/fukusima/pdf/25kome_h26_01.pdf (in Japanese, May 2015)
6. Nemoto K, Abe J (2013) Radiocesium absorption by rice in paddy field ecosystem. In: Nakanishi TM, Tanoi K (eds) Agricultural implications of the Fukushima nuclear accident. Springer, Tokyo, pp 19–27
7. MAFF (2014b) http://www.maff.go.jp/j/kanbo/joho/saigai/fukusima/pdf/yousui_h26_8.pdf (in Japanese, May 2015)
8. Tsumura A et al (1984) Behavior of radioactive Sr and Cs in soils and soil-plant systems. Nat Inst Agro-Environ Sci Rep 36:57–113
9. Tsuruta et al (2014) Long-term changes for the three years of the radioactive material concentration of atmospheric aerosols in Fukushima and its surrounding 3 point. In: Abstracts of the 15th workshop on environmental radioactivity, p1
10. Editorial Boards of Methods for Soil Environment Analysis (1997) Methods for soil environment analysis. Hakubunkan Shinsha Publishers Press, Tokyo
11. Suzuki Y et al (2015) Effect of the concentration of radiocesium dissolved in irrigation water on the concentration of radiocesium in brown rice. Soil Sci Plant Nutr 61:191–199

Chapter 18
Radiocesium and Potassium Decreases in Wild Edible Plants by Food Processing

Keiko Tagami and Shigeo Uchida

Abstract It is more than 4 years since March 11, 2011, and, at this stage, foods that exceed the standard limits of radiocesium are mainly from the wild. Hence, one of the public's main concerns is how to decrease ingestion of radiocesium from foods they have collected from the wild as well as from their home-grown fruits because radioactivities in these food materials have not been monitored. In this study, we focused on wild edible plants and fruits, and the effects of washing, boiling, and pealing to remove radiocesium were observed. Samples were collected in 2013 and 2014 from Chiba and Fukushima Prefectures, e.g., young bamboo shoots, giant butterbur, and chestnuts. Wild edible plants were separated into three portions to make raw, washed, and boiled samples. For fruit samples (i.e., persimmon, loquat, and Japanese apricot), fruit parts were separated into skin, flesh, and seeds.

It was found that washing of plants is not effective in removing both ^{137}Cs and ^{40}K, and that boiling provided different removal effects on plant tissues. The retention factors of ^{137}Cs and ^{40}K for thinner plant body sample (leaves) tended to be higher than those for thicker plant body types, e.g., giant butterbur petiole and bamboo shoots. Thus, the boiling time as well as the crop thickness affects radiocesium retention in processed foods. For fruits, Cs concentration was higher in skin than in fruit flesh for persimmon and loquat; however, Japanese apricot showed different distribution.

Keywords Food processing retention factor • Radiocesium • Potassium • Wild edible plants • Fruits

18.1 Introduction

Radiocesium (^{134}Cs + ^{137}Cs) concentrations in foods are of great concern in Japan since the Fukushima Daiichi Nuclear Power Plant (FDNPP) accident, as people wish to avoid receiving additional internal doses from ingestion of the radionuclide.

K. Tagami (✉) • S. Uchida
National Institute of Radiological Sciences, Anagawa 4-9-1, Inage-ku, Chiba-shi, Chiba 263-8555, Japan
e-mail: k_tagami@nirs.go.jp

T. Takahashi (ed.), *Radiological Issues for Fukushima's Revitalized Future*,
DOI 10.1007/978-4-431-55848-4_18

Food monitoring has been carried out since March 2011; provisional regulation values for total radiocesium concentration were applied at the time, and the values were 200 Bq kg^{-1} for water, milk, and daily products, and 500 Bq kg^{-1} for other food materials. From April 1, 2012, standard values for radiocesium have been employed in Japan, and the concentration in marketed raw food materials has been limited up to 100 Bq kg^{-1}, except baby foods (50 Bq kg^{-1}) and drinking water (10 Bq kg^{-1}). If any food exceeds these limits, the food name together with the producing district has been reported immediately by the Ministry of Health, Labour, and Welfare (MHLW). Every month, radioactivities of more than 20,000 samples are being measured and the recent data of February 2015 [1] have shown that foods exceeding the standard limits were mostly from the wild (i.e., not commercially grown or raised), i.e., meats of wild boar, Sika deer, Asian black bear, Japanese rock fish (marine), Japanese eel and char (freshwater). Not only meats but also edible wild plants in spring and autumn in 2014, e.g., giant butterbur flower-bud, Japanese angelica-tree shoot (*taranome*), and various mushrooms species, exceeded the limits.

One of the public's main concerns is how to decrease ingestion of radiocesium from foods, especially foods they have collected from the wild as well as from their home-grown garden fruits because radioactivities in these foods have not been measured for many cases. Unfortunately, radiocesium removal data by food processing, including culinary preparation, for crops commonly consumed in Japan have been limited because of little interest in the topic before the FDNPP accident. To remedy this, Japanese researchers have begun collecting such data [2–12]. Recently, the Radioactive Waste Management Funding and Research Center (RWMC) compiled the radiocesium removal ratios by food processing using open source data published mainly in 2011 and 2012 [13]. However, it is necessary to add more data to update the information.

In the present study, we focused on food processing effects on radiocesium removal in food plants from the wild to add more information and we compared obtained values with previously compiled values in the IAEA Technical Report Series No. 472 [14]. We also measured potassium-40 (^{40}K) concentrations in the same samples for comparison with radiocesium.

18.2 Materials and Methods

The following samples were collected in Chiba and Fukushima Prefectures in 2013 and 2014: giant butterbur (*Petasites japonicus*: flower-bud, 2; leaf blade, 4; petioles, 4), Japanese mugwort (*Artemisia indica var. Maximowiczii*: young shoots, 4), field-horsetail (*Equisetum arvense*: fertile stem, 3), water dropwort (*Oenanthe javanica*: young shoots, 1), Moso bamboo (*Phyllostachys heterocycla f. pubescens*: young shoots, 8), chestnut (*Castanea crenata*: nuts, 3), persimmon (*Diospyros kaki*: fruits, 2), loquat (*Eriobotrya japonica*: fruits, 4), and Japanese apricot (*Prunus mume*, 1). Sampling dates are listed in Tables 18.1, 18.2, and 18.3. Immediately after the

Table 18.1 Food processing retention factor (F_r) of ^{137}Cs and ^{40}K for giant butterbur tissues collected in 2013–2014

Tissue	Sampling date	Method of processing	Wet mass ratio	F_r of ^{137}Cs	F_r of ^{40}K
Flower bud	2013/3/13	Boiling	1.1	0.19 ± 0.11	0.56 ± 0.10
Flower bud	2013/3/18	Boiling	1.2	0.40 ± 0.18	0.65 ± 0.14
Leaf blade	2013/4/5	Washing	1.0	0.90 ± 0.10	1.24 ± 0.08
Leaf blade	2013/4/19	Washing	1.0	1.01 ± 0.08	1.10 ± 0.07
Leaf blade	2013/4/30	Washing	1.0	1.04 ± 0.08	0.99 ± 0.05
Leaf blade	2014/4/8	Washing	1.0	0.98 ± 0.10	0.99 ± 0.04
Leaf blade[a]	*2012–2014*	*Washing*	–	*0.95 (n = 8)*	*1.02 (n = 8)*
Leaf blade	2013/4/5	Boiling	1.1	0.43 ± 0.05	0.51 ± 0.04
Leaf blade	2013/4/19	Boiling	1.0	0.39 ± 0.03	0.60 ± 0.04
Leaf blade	2013/4/30	Boiling	1.0	0.46 ± 0.04	0.56 ± 0.03
Leaf blade	2014/4/8	Boiling	0.95	0.40 ± 0.05	0.44 ± 0.02
Leaf blade[a]	*2012–2014*	*Boiling*	–	*0.40 (n = 8)*	*0.46 (n = 8)*
Petiole	2013/4/5	Washing	1.0	0.69 ± 0.16	1.20 ± 0.07
Petiole	2013/4/19	Washing	1.0	1.34 ± 0.26	0.90 ± 0.05
Petiole	2013/4/30	Washing	1.0	1.10 ± 0.18	1.01 ± 0.05
Petiole	2014/4/8	Washing	1.0	0.91 ± 0.20	0.94 ± 0.04
Petiole[a]	*2012–2014*	*Washing*	–	*0.97 (n = 8)*	*1.01 (n = 8)*
Petiole	2013/4/5	Boiling	0.83	0.59 ± 0.12	0.82 ± 0.05
Petiole	2013/4/19	Boiling	0.84	0.93 ± 0.18	0.73 ± 0.04
Petiole	2013/4/30	Boiling	0.84	0.66 ± 0.10	0.66 ± 0.03
Petiole[b]	2014/4/8	Boiling	1.0	0.37 ± 0.10	0.35 ± 0.02
Petiole[a]	*2012–2014*	*Boiling*	–	*0.80 (n = 8)*	*0.80 (n = 8)*

$\pm$ shows error from counting

[a]Averaged value for the data collected from 2012 (published in [2]) to 2014

[b]The sample was kept in water for 1 h after boiling

collection, samples were transferred to a laboratory and weighed to obtain the fresh weight.

In order to obtain the food processing effect, giant butterbur, Japanese mugwort, and water dropwort samples were separated into three portions to make raw, washed, and boiled (2.5 min) subsamples. One giant butterbur petiole sample was soaked in water for 1 h at room temperature after boiling. Field horsetail, young bamboo shoot, and chestnut samples were separated into two portions to make raw and boiled subsamples (boiling times depended on samples). All samples were weighed before processing. Washing was carried out with tap water in a washing bowl by changing the water five times, and then, finally, the samples were rinsed with reverse osmosis (RO) water. For the boiling process, edible parts of the plants were cooked in RO water after washing with tap water five times. For fruits, a whole fruit was washed with running tap water and rinsed with RO water. Then the water was removed with paper towels from the fruits, and each tissue part (skin, flesh, and seeds) was separated and weighed.

Table 18.2 Food processing retention factor (F_r) of ^{137}Cs and ^{40}K for eight bamboo shoots collected in 2013

Tissue	Sampling date	Method of processing	Wet mass ratio	F_r of ^{137}Cs	F_r of ^{40}K
New shoot-1	2013/4/9	Boiling	0.97	0.94 ± 0.04	0.80 ± 0.05
New shoot-2	2013/4/9	Boiling	0.95	0.66 ± 0.04	0.67 ± 0.06
New shoot-3	2013/4/9	Boiling	0.95	0.65 ± 0.02	0.55 ± 0.06
New shoot-4	2013/4/9	Boiling	–	0.68 ± 0.03	0.69 ± 0.05
New shoot-5	2013/4/9	Boiling	–	0.65 ± 0.03	0.69 ± 0.04
New shoot-6	2013/4/9	Boiling	0.99	0.67 ± 0.02	0.63 ± 0.06
New shoot-7	2013/4/9	Boiling	0.97	0.88 ± 0.04	0.75 ± 0.06
New shoot-8	2013/4/9	Boiling	0.97	0.79 ± 0.05	0.80 ± 0.07
New shoot[a]	*2012–2013*	*Boiling*		*0.71 (n = 12)*	*0.73 (n = 12)*

± shows error from counting
[a]Averaged value for the data collected from 2012 (published in [2]) to 2013

Table 18.3 Food processing retention factor (F_r) of ^{137}Cs and ^{40}K for mugwort (M), field horsetail (F), water dropwort (W), and chestnut (C) collected in 2013–2014

Tissue	Sampling date	Method of processing	Wet mass ratio	F_r of ^{137}Cs	F_r of ^{40}K
M, New shoots	2013/5/8	Washing	1.0	0.87 ± 0.37	1.14 ± 0.07
M, New shoots	2013/5/24	Washing	1.0	1.09 ± 0.02	0.86 ± 0.13
M, New shoots	2013/9/26	Washing	1.0	0.89 ± 0.03	0.97 ± 0.32
M, New shoots	2014/12/9	Washing	1.0	0.77 ± 0.36	0.97 ± 0.05
M, New shoots[a]	*2012–2014*	*Washing*	–	*0.98 (n = 9)*	*0.97 (n = 9)*
M, New shoots	2013/5/8	Boiling	1.0	0.36 ± 0.21	0.57 ± 0.04
M, New shoots	2013/5/24	Boiling	1.1	0.25 ± 0.01	0.45 ± 0.08
M, New shoots	2013/9/26	Boiling	1.0	0.47 ± 0.02	0.64 ± 0.19
M, New shoots	2014/12/9	Boiling	0.94	0.29 ± 0.20	0.26 ± 0.02
M, New shoots[a]	*2012–2014*	*Washing*	–	*0.39 (n = 8)*	*0.46 (n = 8)*
F, Fertile stem	2013/3/8	Boiling	0.81	0.62 ± 0.29	0.43 ± 0.0.5
F, Fertile stem	2013/3/20	Boiling	0.86	0.47 ± 0.25	0.57 ± 0.08
F, Fertile stem	2013/3/26	Boiling	0.75	0.16 ± 0.33	0.44 ± 0.04
F, Fertile stem[a]	*2012–2014*	*Boiling*	–	*0.46 (n = 6)*	*0.52 (n = 6)*
W, New shoots	2013/5/24	Washing	1.0	0.90 ± 0.06	0.96 ± 0.22
W, New shoots	2013/5/24	Boiling	0.83	0.61 ± 0.04	0.32 ± 0.12
C, nuts-1[b]	2013/9/26	Boiling	1.0	1.30 ± 0.01	1.04 ± 0.17
C, nuts-2[b]	2013/9/26	Boiling	1.0	0.68 ± 0.01	0.78 ± 0.15
C, nuts-3[b]	2013/9/26	Boiling	1.0	0.81 ± 0.01	0.77 ± 0.19

± shows error from counting
[a]Averaged value for the data collected from 2012 (published in [2]) to 2014
[b]Samples taken from different trees

Then, all samples were oven-dried at 80 °C to decrease the sample volume. Each oven-dried sample was pulverized and mixed well, and then transferred to a plastic container (U8 container). Radioactivity concentration in each sample was measured by a Ge detecting system (Seiko EG&G) and the gamma spectrum was analyzed using Gamma Station software (Seiko EG&G) to obtain activity on wet mass basis (Bq kg^{-1}-wet mass). The detection limit was about 0.5–1.0 Bq kg^{-1}-wet mass with the counting time of 40,000–80,000 s. The radiocesium concentrations in samples were usually low and sometimes ^{134}Cs could not be detected 2–3 years after the accident. Therefore, in this study, only ^{137}Cs data are presented together with ^{40}K.

Food processing retention factor (F_r) was determined by using the following equation as defined in IAEA TRS-472 [14]:

$$F_r = A_{after}\,(Bq) \;/\; A_{before}\,(Bq)$$

where A_{after} is the total activity of ^{137}Cs or ^{40}K retained in the food after processing (Bq), and A_{before} is the total activity in the food before processing (Bq). The wet mass of the processed subsample before processing (W_{bp}, kg) was recorded, thus, A_{before} was calculated using the following equation:

$$A_{before} = C_{raw} \times W_{bp}$$

where C_{raw} is the radioactivity concentration of ^{137}Cs or ^{40}K in the raw subsample (Bq kg^{-1}-wet mass).

For fruit samples, distribution percentages of wet mass, ^{137}Cs and ^{40}K in skin, flesh, and seeds were calculated and these distributions were compared.

18.3 Results and Discussion

The F_r values of ^{40}K and ^{137}Cs for each wild edible plant sample are shown in Tables 18.1, 18.2, and 18.3. Some F_r data exceeded 1.0 although that is impossible from the above equation; however, because of the low concentrations in samples giving a large counting error, and the samples for raw and processed samples being not completely the same, values of more than 1.0 were inevitable.

The mean F_rs of ^{137}Cs by washing for butterbur leaf blade ($n = 4$), petiole ($n = 4$), mugwort ($n = 4$), and water dropwort ($n = 1$) were 0.98, 1.0, 0.91, and 0.90, respectively and that of ^{40}K were 1.1, 1.0, 0.98, and 0.96, respectively. From this result, it was clear that washing plants is not effective to remove both ^{40}K and ^{137}Cs, because both elements are distributed inside the plant body. Boiling provided different removal effects by plant tissues. The mean F_rs of ^{137}Cs for leaf-blade of giant butterbur ($n = 4$), mugwort ($n = 4$), water dropwort ($n = 1$), and fertile stem of field horsetail ($n = 3$) were 0.40, 0.41, 0.61, and 0.42, respectively, i.e., about 40–60 % of the ^{137}Cs was removed by this process. Similar results were observed for ^{40}K for these samples. Unfortunately, however, the number of samples treated in 2013–2014 was not enough for statistical analysis between F_rs of ^{40}K and ^{137}Cs in

each plant species. Only analytical results for bamboo shoots ($n = 8$) are reported here; when ANOVA test was carried out, no statistical difference was observed between F_rs of ^{40}K and ^{137}Cs. For some sample types, all the data from 2012 (reported in [2]) to 2014 were summarized (Tables 18.1, 18.2, and 18.3) and the values for ^{40}K and ^{137}Cs did not show any statistical differences by ANOVA test. Thus, we concluded that K could be used as an analogue for radiocesium to calculate F_rs.

Compared to leafy samples, bamboo shoots and petioles of giant butterbur (except soaking in water for 1 h) showed slightly higher F_rs of ^{137}Cs of 0.74 and 0.73, respectively; since these tissues are thicker than leaf tissues, it is reasonable to expect that more radiocesium would be retained in these tissues. However, when the giant butterbur sample soaked in water for 1 h showed lower F_r values, therefore, boiling followed by soaking would effectively remove ^{137}Cs, although K was also removed by this process. For chestnut, mean values of F_r of ^{137}Cs and ^{40}K were 0.95 and 0.87, respectively. Removal of these two elements by boiling of chestnut was difficult, because the hard shell prevented extracting ^{137}Cs and ^{40}K from the nuts into the boiling water. In total, most of the F_r values presented in this study and our previous data [2] were within the range of values compiled by IAEA [14], as shown in Fig. 18.1.

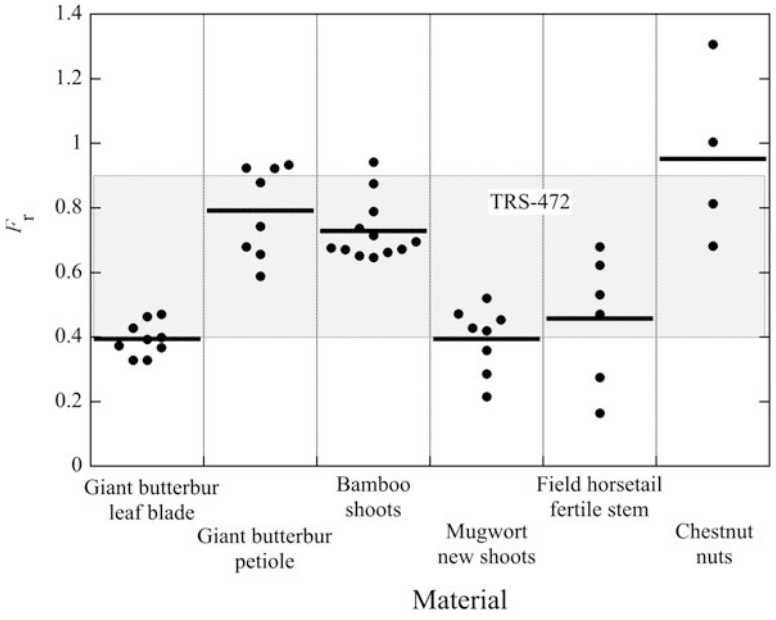

Fig. 18.1 Comparison of food processing retention factor (F_r) of ^{137}Cs for several plant materials collected in 2011–2014 by boiling. Both previous [2] and present study's data are plotted. The *shaded area* shows Fr range for vegetables, berries, and fruits boiled in water reported in TRS-472 by IAEA [14]

Table 18.4 Relative proportions (%) of wet mass, ^{137}Cs and ^{40}K in fruit tissues (skin, flesh, and seeds) to whole fruits for four species collected in 2013–2014 at harvest

Sample	Sampling date	Wet mass, %			^{137}Cs, %			^{40}K, %		
		Skin	Flesh	Seeds	Skin	Flesh	Seeds	Skin	Flesh	Seeds
Persimmon[a]	2011/10/4	13	83	4	23	67	10	–	–	–
Persimmon[a]	2011/10/20	9	91	–	19	81	–	–	–	–
Persimmon	2013/10/8	11	85	4	16	74	11	22	71	7
Persimmon	2014/10/9	11	85	4	16	81	2	19	76	5
Loquat	2011/6/7	22	47	31	34	44	21	–	–	–
Loquat-1[b]	2013/6/19	18	59	22	29	50	21	20	39	41
Loquat-2[b]	2013/6/19	12	69	18	19	69	12	16	50	34
Loquat	2014/6/4	16	62	22	22	56	22	22	43	35
Loquat	2014/6/11	11	68	22	15	72	13	13	48	39
Japanese apricot[c]	2012	12	75	13	12	83	6	–	–	–
Japanese apricot	2014/6/4	17	69	14	11	82	7	22	70	8

[a]Data from [15]
[b]Samples were taken from different trees on the same date
[c]Data from [13]

The results for fruits are listed in Table 18.4. For persimmon and loquat fruits, compared to the relative proportions of skin mass to the total fruits, partitioning percentages of ^{137}Cs and ^{40}K in the skin samples were 1.4–2.2 and 1.2–2.0 times higher, respectively, and those in flesh were 0.8–1.1 and 0.6–0.9, respectively. Thus, ^{137}Cs concentrations in skin were higher than those in flesh for both species. On the other hand, Japanese apricot showed higher percentage of ^{137}Cs distribution than wet mass proportion, although ^{40}K distributions were similar to those of wet mass proportion. In this study, we measured only one sample, however, similar results were obtained in 2012 [13], as listed in the same table.

In 2011, loquat and persimmon fruits were also measured and the ^{137}Cs distribution percentages in skin samples [15] were higher than those observed in 2013 and 2014 for both species. It was assumed that immediately after the ^{137}Cs was taken up through these trees' aboveground parts, it transferred to their growing tissues including the fruits; during development of fruits, fruit flesh mass increases at the middle-late ripening stage [16], but probably ^{137}Cs supply reduced due to the smaller amount of ^{137}Cs uptake through tree surface. By this process, ^{137}Cs distributions in fruit parts differed from those we observed in 2013 and 2014, although more studies are necessary to understand the mechanisms of Cs transfer in fruit trees.

18.4 Conclusions

The effects of washing and boiling of wild edible plants, and peeling of home-grown fruits were studied. It was found that washing plant surface is not effective in removing both ^{40}K and ^{137}Cs, because both elements are in the plant tissues. Food processing retention factor, F_r, decreased by boiling, and the average values ranged from 0.40 to 0.61 for leaf-blade of giant butterbur, mugwort, water dropwort, and fertile stem of field horsetail. Bamboo shoots and petioles of giant butterbur (except soaking in water for 1 h), however, showed slightly higher F_rs of ^{137}Cs of 0.59–0.94, because these tissues are thicker than leaf tissues, and thus, it is reasonable to expect that more radiocesium would be retained in these tissues. For fruits of persimmon and loquat, ^{137}Cs concentrations in skin were higher than those in flesh, but different trend was observed in Japanese apricot. Interestingly, the distributions of ^{137}Cs in skin, flesh, and seeds observed in this study differed from those observed in 2011. The mechanism is not clarified yet; therefore, further studies are necessary to understand the radiocesium transfer to fruits after direct deposition to fruit tree surfaces.

Acknowledgement This work was partially supported by the Agency for Natural Resources and Energy, the Ministry of Economy, Trade, and Industry (METI), Japan.

References

1. Ministry of Health, Labour and Welfare (MHLW) (2015) Monthly report of test results of radionuclide in foods sampled since 01 April 2012 (by date). http://www.mhlw.go.jp/stf/kinkyu/0000045281.html. Accessed 7 Apr 2015
2. Tagami K, Uchida S (2013) Comparison of food processing retention factors of ^{137}Cs and ^{40}K in vegetables. J Radioanal Nucl Chem 295:1627–1634
3. Tagami K, Uchida S, Ishii N (2012) Extractability of radiocesium from processed green tea leaves with hot water: the first emergent tea leaves harvested after the TEPCO's Fukushima Daiichi Nuclear Power Plant accident. J Radioanal Nucl Chem 292:243–247
4. Tagami K, Uchida S (2012) Radiocaesium food processing retention factors for rice with decreasing yield rates due to polishing and washing, and the radiocaesium distribution in rice bran. Radioisotopes 61:223–229
5. Okuda M, Hashiguchi T, Joyo M, Tsukamoto K, Endo M, Matsumaru K, Goto-Yamamoto M, Yamaoka H, Suzuki K, Shimoi H (2013) The transfer of radioactive cesium and potassium from rice to sake. J Biosci Bioeng 116:340–346
6. Goto-Yamamoto N, Koyama K, Tsukamoto K, Kamigakiuchi H, Sumihiro M, Okuca M, Hashiguchi T, Matsumaru K, Sekizawa H, Shimoi H (2014) Transfer of cesium and potassium from grapes to wine. Am J Enol Viticult 65:143–147
7. Nabeshi H, Tsutsumi T, Hachisuka A, Matsuda R (2013) Variation in amount of radioactive cesium before and after cooking dry shiitake and beef. Food Hyg Safe Sci 54:65–70

8. Nabeshi H, Tsutsumi T, Hachisuka A, Matsuda R (2013) Reduction of radioactive cesium content in beef by soaking in seasoning. Food Hyg Safe Sci 54:298–302
9. Nabeshi H, Tsutsumi T, Hachisuka A, Matsuda R (2013) Reduction of radioactive cesium content in pond smelt by cooking. Food Hyg Safe Sci 54:303–308
10. Hachinohe M, Naito S, Akashi H, Todoriki S, Matsukura U, Kawamoto S, Hamamatsu S (2015) Dynamics of radioactive cesium during noodle preparation and cooking of dried Japanese udon noodles. Nippon Shokuhin Kagaku Kogaku Kaishi 62:56–62
11. Sekizawa H, Yamashita S, Tanji K, Okoshi S, Yoshioka K (2013) Reduction of radioactive cesium in apple juice by zeolite. Nippon Shokuhin Kagaku Kogaku Kaishi 60:212–217
12. Sekizawa H, Yamashita S, Tanji K, Yoshioka K (2013) Dynamics of radioactive cesium during fruit processing. Nippon Shokuhin Kagaku Kogaku Kaishi 60:718–722
13. Radioactive Waste Management Funding and Research Center (2013) Removal of radionuclide by food processing – radiocesium data collected in Japan. In: Uchida S (ed) RWMC-TRJ-13001-2, RWMC, Tokyo (in Japanese)
14. International Atomic Energy Agency (2010) Handbook of parameter values for the prediction of radionuclide transfer in terrestrial and freshwater environments. Technical report series no.472, IAEA, Vienna
15. Tagami K, Uchida S (2014) Concentration change of radiocaesium in persimmon leaves and fruits – observation results in 2011 spring −2013 summer. Radioisotopes 63:87–92
16. Arai N (2004) Fruit forms and development. In: Yamazaki K, Kubo Y, Nishio T, Ishihara K (eds) Encyclopedia of agriculture. Yokendo, Tokyo, pp 1122–1123 (in Japanese)

Chapter 19
Monte Carlo Evaluation of Internal Dose and Distribution Imaging Due to Insoluble Radioactive Cs-Bearing Particles of Water Deposited Inside Lungs via Pulmonary Inhalation Using PHITS Code Combined with Voxel Phantom Data

Minoru Sakama, Shinsaku Takeda, Erika Matsumoto, Tomoki Harukuni, Hitoshi Ikushima, Yukihiko Satou, and Keisuke Sueki

Abstract The role of this study in terms of health physics and radiation protection has been implemented to evaluate the internal dose (relative to the committed equivalent dose) and the dose distribution imaging due to gamma rays (photons) and beta particles emitted from the radioactive Cs-bearing particles in atmospheric aerosol dusts deposited in the lungs via pulmonary inhalation. The PHITS code combined with voxel phantom data (DICOM formats) of human lungs was used. We have dealt with the insoluble radioactive Cs-bearing particles of water (about ϕ 2.6 μm diameter) migrated onto any of six regions, ET1, ET2, BB, AI-bb, LNET, and LNTH, in a respiratory system until dropping into blood vessels. Source parameters were those of an adult male breathing a typical air volume outdoors; in the simulated atmosphere (such as systematically setting up a field) those particles would be released on 21:10 March 14 to 9:10 March 15, 2011 in Tukuba, Japan,

M. Sakama (✉)
Department of Radiation Science and Technology, Institute of Biomedical Sciences, Tokushima University Graduate School, Kuramoto-cho 3-18-15, Tokushima, Japan
e-mail: minorusakama@tokushima-u.ac.jp

S. Takeda • E. Matsumoto
Department of Radiation Science and Technology, Institute of Biomedical Sciences, Tokushima University Graduate School, Tokushima, Japan

T. Harukuni • H. Ikushima
Department of Therapeutic Radiology, Institute of Biomedical Sciences, Tokushima University Graduate School, Tokushima, Japan

Y. Satou • K. Sueki
Faculty of Pure and Applied Science, University of Tsukuba, Tsukuba, Japan

T. Takahashi (ed.), *Radiological Issues for Fukushima's Revitalized Future*,
DOI 10.1007/978-4-431-55848-4_19

as a filter sampling condition already reported by Adachi et al. In this chapter, we discuss the internal dose and the dose distribution imaging in each voxel phantom for human lung tissues corresponding to the respiratory tracts of BB and AI-bb, respectively.

Keywords Monte Carlo simulation • Committed equivalent dose • Cesium-134 • Cesium-137

19.1 Introduction

At 14:46 JST (Japan Standard Time) March 11th, 2011, a huge earthquake (magnitude Ms = 9.0 at the epicenter; epicenter depth is about 10 km) occurred at sanriku off the coast of eastern Japan. A Great tsunami followed the earthquake and caused serious accidents at the Fukushima Daiichi Nuclear Power Plant (FDNPP) and plant workers had been unable to control the cooling system of nuclear fuels at all the plants 1, 2, 3, and 4. At that time, great amounts of hydrogen gases had been produced around their nuclear fuel rods and the remaining fuel assemblies had not cooled off, filling the plants with hydrogen gases; after a while the emergency condition caused hydrogen explosions at plants 1 (on March 12, 2011) and 3 (on March 14, 2011), and fires also occurred at plants 2 and 4 due to those explosions. These serious accidents had caused the release of large amounts of radioactive materials into the environment together with plumes.

A few years after this accident, we had slightly understood some findings regarding all the radioactivity for released radioactive cesium isotopes of Cs-134 and Cs-137 into the environment and the exact migrations for the radioactive plumes including those radioactive materials upon atmospheric conditions [1–5]. Four years elapsed and it has now become clear that the radioactive materials have chemical and physical properties concerning chemical forms, particle sizes, shape, phases (gas or aerosol), water solubility, and residence time [6–10]. Adachi et al. [11] reported that they directly observed spherical Cs-bearing particles emitted during a relatively early stage (March 14–15) of the accident, and also stated that the spherical Cs-bearing particles were larger (their diameters were approximately 2 μm), and they were less water soluble than sulfate particles. In their report, they investigated the coexistence of spherical Cs-bearing particles with Fe, Zn, and possible other elements using SEM and EDS mapping images with the elemental analysis spectrum.

In addition, Satou et al. [12] similarly reported that they investigated whether specific particles such as the spherical Cs-bearing particles observed by Adachi et al. were included in soil samples at the northwestern area about 20 km away from FDNPP where radioactive plumes migrated on March 15, 2011. It was found that their soil samples contained the same spherical Cs-bearing particles indicated by Adachi et al. [11] and their observed particle size and contained elements were about 2 μm diameter with Fe, Zn, and Rb using the same SEM and EDS analyses; they concluded that their obtained properties of these particles in the soil samples were consistent with those reported by Adachi et al. [11]

As some experimental uptakes allow us to understand step by step the chemical and physical properties of the released radioactive Cs-suspending materials taking forms such as spherical Cs-bearing particles into the plumes, we consider that there exists a need to estimate the health effects on the large crowd of people who were outside around FDNPP or away from there when the plumes migrated after the accident. In the course of this research regarding health physics, we have offered some evaluation materials for the health effects based on calculation of the internal dose and the dose distribution imaging due to beta particles and photons emitted from the Cs-bearing particles deposited inside the lungs in pulmonary inhalation using the PHITS ver. 2.76 (Particle and Heavy Ion Transport code System) code [13] combined with voxel phantom data [14] (formed by the DICOM format) of a human lung next to human respiratory tracts.

In the present work, taking source parameters on the calculation includes the radioactive Cs-bearing particles (about ϕ 2.6 μm diameter) distributed onto each of six regions, ET1, ET2, BB, AI-bb, LNET, and LNTH, in a human respiratory tract group until dropping into blood vessels on the assumption of one adult male breathing a typical air volume outdoors during March 14, 21:10 (local time) to March 15, 09:10, 2011 in Tukuba, Japan [11]. We have evaluated the internal exposure and the dose distribution imaging in each of the lung voxel phantoms corresponding to the regions of BB and AI-bb, respectively, using the PHITS code. The period of our interest includes an aerosol sampling filter with a maximum radioactivity level of about 1.00E+04 mBq/m^3 from the radioactive plume and also the radioactive Cs-bearing spherical particles found in the filter, as reported by Adachi et al. [11].

19.2 Method and Materials

Considering internal exposure results from intake of an unsealed radioactive material, in this case treated as the radioactive Cs-bearing particles of Cs-134 and Cs-137, to the human body, it seems natural that there are three pathways into the body for the radioactive material to take:

1. Inhalation: entry through organs in a respiratory tract
2. Ingestion: entry through gastrointestinal tract
3. Direct absorption: absorption through intact or wound

It should be noted that the inhalation pathway is most closely connected with a suspending material such as an aerosol cluster in the atmosphere. In the human body, the respiratory tract is mainly in charge of inhalation. To estimate internal exposure at each of the organs or tissues using all calculation methods such as Monte Carlo simulation codes, there is a need for appropriate mathematical models to describe the various processes involved in the internal deposition and retention of the cesium nuclides and the associated radiation doses of gamma rays (photons) and beta particles emitted from these decays received by various organs and tissues

in the respiratory tract. As a general standard model, the respiratory tract is viewed as a series of compartments into which the cesium-bearing particles enter and exit at various rates, ultimately being removed from the respiratory tract regions through exhalation and mechanical clearance processes to outside the body, gastrointestinal tract, and blood, respectively. We have stated here that a deposited dose at each organ or tissue, which is due to various radiation, should really be equivalent to a "committed equivalent dose" including the well-known one of radiation safety terms. That is, in this study, the committed equivalent dose should be estimated extremely at each compartment composed of respiratory tract regions using the PHITS code based on a Monte Carlo calculation method.

Following the recommendations by the ICRP in publication 60 [15] and the model of the human respiratory tract in publication 66 [16], we had properly specified PHITS calculation parameters in input files on which geometrical definitions of PHITS's own code (so-called PHITS language) were interpreted as compartment models of the human respiratory tracts. This compartment modeling was conformed for children aged 3 months, 1, 5, and 10 years and for male and female 15-year-olds and adults of a general population stated on the ICRP publications. The respiratory tract regions were represented by five regions: the Extrathoracic (ET) airways were divided into ET1, the anterior nasal passage, and ET2, consisting of the posterior nasal and oral passages, the pharynx and larynx. The thoracic regions were Bronchial (BB), Bronchiolar (bb), and Alveolar-Interstitial (AI, the gas exchange region). For the bb and AI, inasmuch as both are located next to each other around respiratory terminal bronchioles, in this study we regarded them as a unity region of AI+bb. Lymphatics were associated with the extrathoracic and thoracic airways (LNET and LNTH). Their regions were defined based principally on radiobiological considerations, but also taking account of differences in respiratory function, deposition, and clearance for the generation member. Each PHITS calculation at those six regional compartments, ET1, ET2, BB, AI-bb, LNET, and LNTH, was implemented by 100,000 histories of photon (gamma ray) and beta particle (e^-) decaying Cs-134 and Cs-137 nuclides, respectively, with three different types, type-F (fast), type-M (middle), and type-S (slow), of cesium transfer coefficients into a respiratory tract in a body, assuming that the radioactive Cs-bearing particles (2.6 μm diameter) were deposited at each tissue of those six tissue region compartments. The transfer coefficients were obtained by the WinAct package software [17] based on the ICRP publication 66. This package software is the ORNL numerical solver (Windows version) for the coupled set of differential equations describing the kinetics of a radionuclide in the body.

With the present PHITS calculation method of the committed equivalent doses due to the Cs-bearing particles on the respiratory tract regions, it is very important to evaluate U(50) and SEE (Specific Effective Energy) values. U(50) gives the total number of decaying nuclides which depends on the decay property and the elemental transfer coefficient into a tissue of interest and the value has been

evaluated using the WinAct software. Setting three types of differences in transfer coefficients from type-F to type-M and type-S, we have estimated the committed equivalent doses upon the three cesium transfer conditions on each type of U(50). SEE values have the relationship among radiation branching ratios, Y, radiation energies for gamma rays and average beta particles of Cs-134 and Cs-137, E, specific absorbed fraction, SAF, and radiation weighting factor, w, and this value is given in the function:

$$\mathrm{SEE} = Y \times E \times \mathrm{SAF} \times w. \tag{19.1}$$

The general standard method includes the general committed equivalent dose that thus far has been estimated using the SEE value based on the empirically recommended SAF value of ICRP publication 66. Using the present PHITS calculation method, its code has provided the committed equivalent dose on which the PHITS output data directly result in a relative specific absorbed dose per a radiation source event (Gy/source). Therefore, as it is strongly confirmed that it should correspond to the fraction of SAF as shown in Eq. (19.1), the SEE value can be given as involving the SAF value, and we are consequently able to provide the committed equivalent doses (Sv/particles) for each respiratory tract using the SEE involved on the calculated SAF value, Y, and w in Eq. (19.1).

This PHITS code simulates initial beta and gamma decay properties [18] emitted from Cs-134 and Cs-137 nuclides into the Cs-bearing particles and secondary radiation associated their radiation event by event in a virtualized space. The input files include voxel phantom data compiled for PHITS code into which it has given geometrical and material information of the respiratory tracts and source information of the initial radiations generated uniformly at each respiratory tract of interest as a source region. In other words, the committed equivalent dose has also been provided with the summation of absorbed doses on a lung tissue event by event into a compartment respiratory tract model by adding U(50) and radioactivity ratio (a ratio of about one to one; this is experimentally well-known from many reports of investigations of specific radioactivity for various environmental samples) of Cs-134 and Cs-137 at an early stage of this nuclear accident to the PHITS input data.

For the present treatment of voxel computational phantoms referred to the adult reference male of ICRP 110 publication [19] we have compiled its CT values [20] formed by the DICOM format to the PHITS input data using the "dicom2phits" package program combined with the PHITS calculation code. This program has involved the data exchange functions based on the relationship between CT values [19, 20] and material densities and compositions at each tissue or organ [14]. In the present PHITS input file, we have generated the voxel phantom data with the smallest unit size of $0.98 \times 0.98 \times 10\,\mathrm{mm}^3$ for each compartment of the respiratory tract regions around a human lung.

19.3 Results

19.3.1 U(50): Total Number of Decaying Nuclides at Respiratory Tracts of BB and AI

Table 19.1 summarized the total numbers U(50) of decaying Cs-134 and Cs-137 nuclides at respiratory tracts of BB and AI in comparison with their three different types, type-F (fast), type-M (middle), and type-S (slow). Both the BB and AI tissues shown in Table 19.1, indicate that their U(50) values of type-S (small) for Cs-134 and Cs-137 should become obviously highest with a decreasing cesium transfer coefficient so that the cesium elements have been deposited at each respiratory tract for a long time. In particular, there is a very remarkable difference among the type-F, type-M, and type-S at the AI respiratory tract due to the very large surface area of small alveoli around respiratory bronchioles.

19.3.2 Internal Exposure Dose Distribution Imaging for a Respiratory Tract of BB

Figure 19.1a shows the whole systematic upper half of the human body constructed from the voxel phantom data compiled by the PHITS language. The geometrical and material voxel phantom data around a lung are described based on phantom data of an adult male with CT value using the "dicom2phits" package program combined with the PHITS calculation code. The other figures illustrate the calculated internal exposure dose distributions (expressed at the vertical axis of the absorbed dose (Gy) at T-heat mode on PHITS) of type-S in Fig. 19.1b and type-F in Fig. 19.1c for the BB respiratory tract of the present interest. Their absorbed doses expressed into the figures contribute to whole radiation energies absorbed at each tissue due to the primary gamma rays emitted from Cs-134 and Cs-137 decaying nuclides at the BB respiratory tract. The figures represent that both distributed intensities of absorbed dose for type-S and type-F have increased as formed outlines of the compartment boundaries of BB respiratory tract because of the radiation source generation in there. In addition, in comparison between the figures, it has been found that both generated radiation has been gradually transported on the same order of about 10^3–10^4 as the intensity distributions across the entire upper half of the body. And

Table 19.1 The total numbers of decaying Cs-134 and Cs-137 nuclides at respiratory tracts of BB and AI

	Cs-134			Cs-137		
Tissue	Type-F	Type-M	Type-S	Type-F	Type-M	Type-S
AI	275.17	2843600	10958000	271.85	3186500	23961000
BB	22.936	57487	73884	22.659	58184	75069

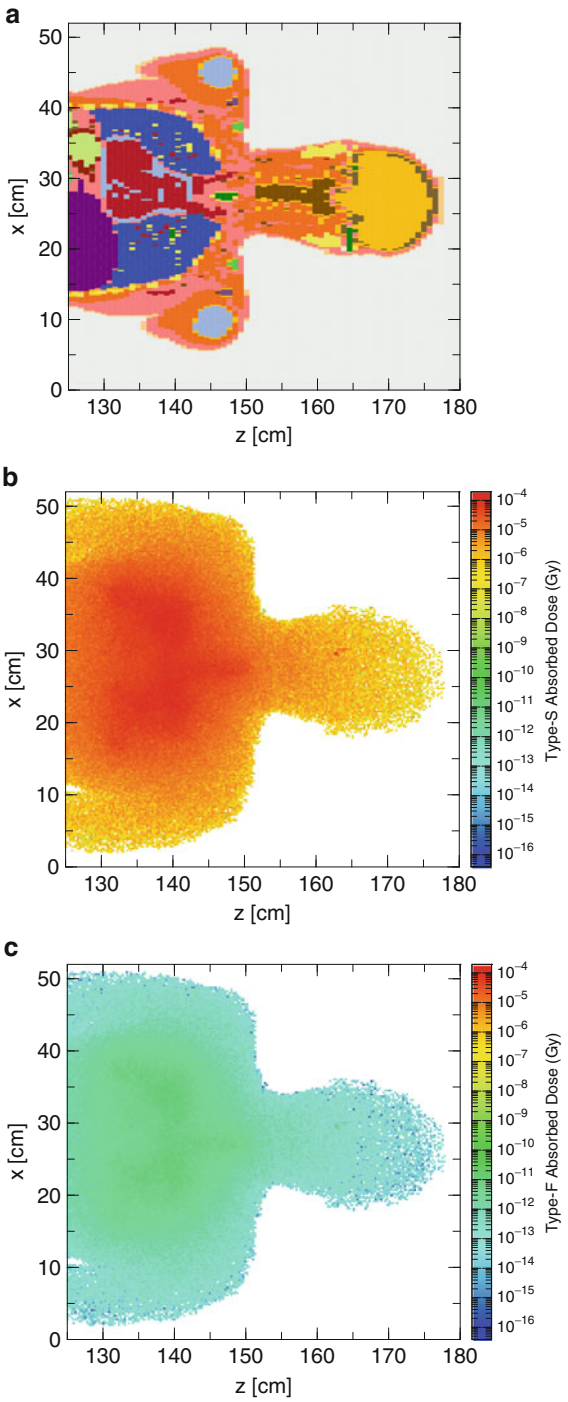

Fig. 19.1 (**a**) Shows the entire systematic upper half of the human body constructed from the voxel phantom data compiled by PHITS language. (**b**, **c**) Illustrate the calculated internal exposure dose distributions expressed at the vertical axis of absorbed dose (Gy) obtained from T-heat results on PHITS

also the absorbed dose distribution of type-S was much higher than that of type-F, because it is definitely likely that it was caused by the total number U(50) of type-S more than that of type-F into the BB region due to too many extremely late Cs-134 and Cs-137 nuclides transferring in the region upon the transfer coefficients of type-S to the blood and gastrointestinal tract.

19.3.3 Committed Equivalent Doses in Comparison with Dependence on Gamma Rays and Beta Particles Between Cs-134 and Cs-137

Tables 19.2 and 19.3 show calculated committed equivalent doses in a comparison with dependence on gamma rays and beta particles associated with the decaying nuclides of Cs-134 and Cs-137 between two methods of PHITS and the general standard method, and also among transfer coefficients of type-F, type-M, and type-S, respectively. In this chapter, we have focused on the calculated result data in a comparison between BB and AI+bb respiratory regions. Comparing all the factors of radiation, transfer coefficient, and respiratory tract in our obtained data as shown in Tables 19.2 and 19.3, it is very likely that the present PHITS simulated method can reproduce those committed equivalent doses estimated approximately by the general standard method. Especially, it is really remarkable that the committed equivalent

Table 19.2 Comparison with calculated committed equivalent doses of Bronchial (BB) and a unity region of Alveolar-Interstitial (AI) and Bronchiolar (bb), which are associated with gamma rays of Cs-134 and Cs-137, by PHITS and general standard method

		Cs-134: gamma ray (Sv/particles)			Cs-137: gamma ray (Sv/particles)		
		Type-F	Type-M	Type-S	Type-F	Type-M	Type-S
PHITS	BB	2.85602E-11	4.26206E-08	1.57344E-07	1.60146E-11	1.86545E-08	1.43411E-07
	AI+bb	2.56911E-11	3.74353E-08	1.41104E-07	1.30911E-11	1.71161E-08	1.29311E-07
General standard method	BB	3.34002E-11	3.95500E-08	1.45290E-07	1.32564E-11	1.78343E-08	1.36558E-07
	AI+bb	2.73125E-11	3.76565E-08	1.41924E-07	1.08211E-11	1.70816E-08	1.28834E-07

Table 19.3 Comparison with calculated committed equivalent doses of Bronchial (BB) and a unity region of Alveolar-Interstitial (AI) and Bronchiolar (bb), associated with beta particles of Cs-134 and Cs-137, by PHITS and general standard method

		Cs-134: β-particle (Sv/particles)			Cs-137: β-particle (Sv/particles)		
		Type-F	Type-M	Type-S	Type-F	Type-M	Type-S
PHITS	BB	1.62220E-11	2.18575E-08	4.03264E-08	1.71321E-11	1.06724E-06	7.89293E-06
	AI+bb	7.15408E-12	6.32775E-08	2.40142E-07	8.40650E-12	8.73540E-08	6.46041E-07
General standard method	BB	4.21726E-10	4.60743E-07	6.01231E-07	5.86399E-10	6.60018E-07	9.03500E-07
	AI+bb	1.94080E-11	7.51489E-08	2.45339E-07	2.66325E-11	1.02437E-07	6.11277E-07

doses attributed to the gamma rays of Cs-134 and Cs-137 on the PHITS calculation results are entirely consistent with those of the general standard method at both the respiratory tracts of BB and AI+bb.

19.4 Discussion

In the present study, providing that the radioactive Cs-bearing particles around 21:00 March 14 to 9:00 March 15, 2011, which were probably released from the FDNPP at the early stage of the nuclear accident, are supposed to have been deposited into human lung tissues from the main to tip regions corresponding to BB and AI+bb respiratory tracts, we have discussed that the PHITS method [13] would probably be available for a Monte Carlo evaluation of committed equivalent dose and the relative internal dose distribution imaging based on possible systematic and optional arrangements using the human voxel phantom by itself or a nearby generation, for example, Japanese adult Male (JM) voxel phantom [14], for anyone with health concerns in Fukushima.

Through a course of the present PHITS Monte Carlo simulation method that has calculated the deduced committed equivalent doses for several respiratory tracts using voxel phantom data of adult human lung tissues and the absorbed dose distribution imaging due to gamma rays and beta particles, the Cs-bearing particles, we have confirmed that the calculated committed equivalent doses contributed to the gamma rays of Cs-134 and Cs-137 can fairly reproduce these results led by the general standard method as shown in Table 19.2. From the absorbed dose distribution in Fig. 19.1b, considering that it is very likely that the Cs-bearing particles with less water solubility would belong to the transfer coefficient for Type-S, it should be noted that transmitted gamma rays from the BB respiratory tract influence part of the radiation energies on surrounding tissues with a decreasing two to three orders of absorbed dose magnitude of BB itself per voxel into the upper half of the body. In regard to beta particles attributed to Cs-134 and Cs-137 in the Cs-bearing particles at both the BB and AI+bb respiratory tracts, as shown in Table 19.3, those committed equivalent doses evaluated by PHITS are inconsistent with those calculated from general standard method for any type, in particular for Type-S, in comparison with the case of the gamma rays. The difference can be explained by the incorrect exchange of all the actual tissue sizes into AI+bb regions to PHITS input data because CT values in the present DICOM data have a minimum-limited unit size for shaping information of these tracts. And thus, the minimum-limited size would be larger than the actual tissue size and it is very likely that there are wide opening spaces between each of the tissues into the AI+bb regions. We have, therefore, deduced that the present PHITS calculation could not reproduce the transport simulations of beta particles for Cs-134 and Cs-137 due to charged beta particles whose property is definitely involved in the stopping power higher than that of non charged gamma rays, and thus the beta particle may be attributed to be greatly influenced by the difference of each opening space size

around AI+bb. Then, the rate of transmitting beta particles would increase without these energy losses at AI+bb regions where they should lose the radiation energies themselves.

From the viewpoint of Monte Carlo evaluation of the internal dose and the distribution imaging due to the insoluble radioactive Cs-bearing particles of water deposited in the lung tissues of a human (adult male) via pulmonary inhalation around 21:00 March 14 to 9:00 March 15, 2011, this work will bear out that the PHITS method was able to evaluate that the committed equivalent dose of BB is 1.57344E-07 (Sv/particles) and 4.03264E-08 (Sv/particles) associated with gamma rays and beta particles of Cs-134, 1.43411E-07 (Sv/particles), and 7.89293E-06 (Sv/particles) associated with gamma rays and beta particles of Cs-137, respectively, at Type-S reproducing the migration next to an actual transfer coefficient into lung tissues of the simulated adult male person. Additionally, we have found that the PHITS method is primarily available not only for evaluating the distribution of internal doses of any tissues of interest relative to both the absorbed doses and the committed equivalent doses, but also investigating their doses at any small piece such as a voxel level depending on CT value and taking the gamma ray and beta particle specific spectra to elucidate the dose distribution mechanism in detail; we also have stated that there is a need to improve the time-consuming and statistical precision contributing to more correct calculations using the PHITS code in the future.

19.5 Conclusion

We have shown that the present PHITS code, which is combined with voxel phantom data of human lung tissues for an adult male, can approximately evaluate the internal dose relative to the committed equivalent dose and the distribution imaging due to gamma rays and beta particles associated with decaying Cs-134 and Cs-137 at the insoluble radioactive Cs-bearing spherical particles of water probably released during 21:10 March 14 to 9:10 March 15, 2011 in Tukuba, Japan, as reported by Adachi et al. In particular, it was found that the calculated committed equivalent doses due to the gamma-rays of Cs-134 and Cs-137 were entirely consistent with those of the general standard method at both the respiratory tracts of BB and AI+bb using the SEE value based on ICRP publication 66, and the estimated committed equivalent doses were 1.57344E-07 (Sv/particles) and 1.41104E-07 (Sv/particles) for Cs-134 and 1.43411E-07 (Sv/particles) and 1.29311E-07 (Sv/particles) for Cs-137 on both Type-S conditions such as a specific transfer coefficient corresponding to the migration rate of cesium until dropping into blood vessels around lung tissues. The PHITS code will probably be available for evaluation of committed equivalent dose and the relative internal dose distribution imaging based on possible systematic and optional arrangements using the human voxel phantom by itself or nearby generation for anyone with health concerns in Fukushima. We plan in the near future to improve several issues of the time-consuming and statistical errors in order to implement more correct calculations by the PHITS method and to extend this method to

voxel phantom data of the entire human body including various public fields in the environment using the PHITS code coupled with MCAM and RVIS [21].

Acknowledgements The authors are grateful to research group members for radiation transport analysis in Japan Atomic Energy Agency (JAEA), Dr. K. Manabu, Dr. K. Satou, Dr. S. Hashimoto, Dr. T. Furuta, and Dr. T. Satou, for operating voxel phantom data in extremely large file sizes for an adult male and also for implementing the PHITS calculations again and again to make an attempt to optimize the calculation method.

References

1. Manolopoulou M, Vagena E, Stoulos S, Ioannidou A, Papastefanou C (2011) Radioiodine and radiocesium in Thessaloniki, Northern Greece due to the Fukushima nuclear accident. J Environ Radioact 102:796–797
2. Amano H, Akiyama M, Chunlei B, Kawamura T, Kishimoto T, Kuroda T, Muroi T, Odaira T, Ohta Y, Takeda K, Watanabe Y, Morimoto T (2012) Radiation measurements in the Chiba Metropolitan area and radiological aspects of fallout from the Fukushima Dai-ichi nuclear power plants accident. J Environ Radioact 111:42–52
3. Momoshima N, Sugihara S, Ichikawa R, Yokoyama H (2012) Atmospheric radionuclides transported to Fukuoka, Japan remote from the Fukushima Dai-ichi nuclear power complex following the nuclear accident. J Environ Radioact 111:28
4. Katata G, Chino M, Kobayashi T, Terada H, Ota M, Nagai H, Kajino M, Draxler R, Hort MC, Malo A, Torii T, Sanada Y (2015) Detailed source term estimation of the atmospheric release for the Fukushima Daiichi nuclear power station accident by coupling simulations of an atmospheric dispersion model with an improved deposition scheme and oceanic dispersion model. Atmos Chem Phys 15:1029–1070
5. Haba H, Kanaya J, Mukai H, Kambara T, Kase M (2012) One-year monitoring of airborne radionuclides in Wako, Japan, after the Fukushima Dai-ichi nuclear power plant accident in 2011. Geochem J 46:271–278
6. Doi T, Masumoto K, Toyoda A, Tanaka A, Shibata Y, Hirose K (2013) Anthropogenic radionuclides in the atmosphere observed at Tsukuba: characteristics of the radionuclides derived from Fukushima. J Environ Radioact 122:55–62
7. Miyamoto Y, Yasuda K, Magara M (2014) Size distribution of radioactive particles collected at Tokai, Japan 6 days after the nuclear accident. J Environ Radioact 132:1–7
8. Kaneyasu N, Ohashi H, Suzuki F, Okuda T, Ikemori F (2012) Sulfate Aerosol as a potential transport medium of radiocesium from the Fukushima nuclear accident. Environ Sci Technol 46:5720–5726
9. Niimura N, Kikuchi K, Tuyen ND, Komatsuzaki M, Motohashi Y (2015) Physical properties, structure, and shape of radioactive Cs from the Fukushima Daiichi nuclear power plant accident derived from soil, bamboo and shiitake mushroom measurements. J Environ Radioact 139:234–239
10. Yanaga M, Oishi A (2015) Decontamination of radioactive cesium in soil. J Radioanal Nucl Chem 303:1301–1304
11. Adachi K, Kajino M, Zaizen Y, Igarashi Y (2013) Emission of spherical cesium-bearing particles from an early stage of the Fukushima nuclear accident. Sci Rep 3:2554:1–5

12. Satou Y, Sueki K, Sasa K, Kitagawa J, Ikarashi S, Kinoshita N (2015) Vertical distribution and formation analysis of the ^{131}I, ^{137}Cs, ^{129m}Te, and ^{110m}Ag from the Fukushima Dai-ichi nuclear power plant in the beach soil. J Radioanal Nucl Chem 303:1197–1200
13. Sato T, Niita K, Matsuda N, Hashimoto S, Iwamoto Y, Noda S, Ogawa T, Iwase H, Nakashima H, Fukahori T, Okumura K, Kai T, Chiba S, Furuta T, Sihver L (2013) Particle and heavy ion transport code system, PHITS, version 2.52. J Nucl Sci Technol 50:913–923
14. Sato K, Noguchi H, Emoto Y, Koga S, Saito K (2007) Japanese adult male voxel phantom constructed on the basis of CT images. Radiat Prot Dosimetry 123(3):337–344
15. International Commission on Radiological Protection (1991) 1990 recommendations of the international commission on radiological protection. Publication 60. Annals of the ICRP, vol 21/1–3. Pergamon Press, Oxford
16. International Commission on Radiological Protection (1994) Human respiratory tract model for radiological protection. Publication 66. Annals of the ICRP, vol 24/1–3. Pergamon Press, Oxford
17. Leggett RW et al (1993) An elementary method for implementing complex biokinetic models. Health Phys 64:260–278
18. Firestone RB, Shirley VS (eds) (1996) Table of isotopes, 8th edn. Wiley, New York
19. International Commission on Radiological Protection (2009) 1990 adult reference computational phantoms. Publication 110. Annals of the ICRP, vol 39/2. Pergamon Press, Oxford
20. Schneider W (2000) Correlation between CT numbers and tissue parameters needed for Monte Carlo simulations of clinical dose distributions. Phys Med Biol 45:459–478
21. Wu Y, FDS Team (2009) CAD-based interface programs for fusion neutron transport simulation. Fusion Eng Des 84:1987–1992

Chapter 20
A Study of a Development of Internal Exposure Management Tool Suited for Japanese Diet Behavior

Shin Hasegawa, Shinya Oku, Daisuke Fujise, Yuki Yoshida, Kazuaki Yajima, Yasuo Okuda, Thierry Schneider, Jacques Lochard, Isao Kawaguchi, Osamu Kurihara, Masaki Matsumoto, Tatsuo Aono, Katsuhiko Ogasawara, Shinji Yoshinaga, and Satoshi Yoshida

Abstract After the Fukushima Nuclear Power Plant accident, one of the main issues at stake was the potential intake of contaminated foodstuff by residents of the affected areas. In this context, the importance of the management of the internal exposure by food intake has emerged. For this purpose, a system was developed for estimating the amount of the radioactivity ingested through the diet in order to manage the internal exposure evolution of exposed people. The ultimate goal of this system is to consider all the radiation exposure data including medical exposure in an integrated manner.

In this perspective, a tool that was used for internal exposure assessment in Europe after the Chernobyl disaster has been adapted to be suitable to Japanese diet behavior. The tool was implemented in a Web application in order to estimate the amount of radioactivity in the dish and to manage the internal exposure history of the individuals. This system automatically collects the test results of radionuclide in foods available on the web.

It manages the individual internal exposure history estimating the amount of radioactivity in the ingested dish. The developed application enables individual to manage his/her protection by checking radioactivity ingestion history and

S. Hasegawa (✉) • D. Fujise • Y. Yoshida • K. Yajima • Y. Okuda • I. Kawaguchi • O. Kurihara • M. Matsumoto • T. Aono • S. Yoshinaga • S. Yoshida
National Institute of Radiological Sciences, 4-9-1, Anagawa, Inage-ku, Chiba City, Chiba Prefecture, Japan
e-mail: haseshin@nirs.go.jp

S. Oku
Regle Co. Ltd., Fukuro-machi, Shinjuku-ku, Tokyo, Japan

T. Schneider • J. Lochard
Nuclear Evaluation Protection Centre (CEPN), 28 Rue de la Redoute, 92260 Fontenay-aux-Roses, France

K. Ogasawara
Faculty of Health Sciences, Hokkaido University, N12-W5, Kitaku, Sapporo, Japan

T. Takahashi (ed.), *Radiological Issues for Fukushima's Revitalized Future*,
DOI 10.1007/978-4-431-55848-4_20

determining to eat or not the dish according to the amount of radioactivity in the dish. This system, which has the potential to contribute to the radiation protection culture of people living in the contaminated areas of Fukushima Prefecture, has been evaluated by specialists of radiation protection. The following step will be the test of the system by the individuals themselves.

Keywords Internal exposure management • Internal exposure from food intake • Radioactivity ingestion history management • Radiation protection culture

20.1 Introduction

A large amount of radioactive materials was released into the environment by the Fukushima Daiichi nuclear power plant accident caused by the Great East Japan Earthquake, leading to an increasing concern of the citizens about radiation. As a result, not only the concern about the external radiation exposure from the environment but also the growing concern about internal radiation exposure related to food deepened awareness of the importance of a global exposure dose management. It is the purpose of this research to handle and to unify the information about the radiation exposure for affected individuals.

According to ICRP Publication 111 [1], optimization of radiation protection for the residents living in the contaminated areas is the driving principle. This cannot be achieved without engaging the affected people in the process and in this perspective information and dialogue meetings on radiation protection, and a variety of lectures have been carried out [2]. Upon preliminary investigation of the present study, the authors participated in dialogue meetings, which took place in the affected areas. This was an opportunity to hear the voice of the residents. What we learned was that many people in the absence of measurements related to their own situation were anxious about the situation and as a result had no other choice than imposing themselves restrictions in their diet. This was perceived as a strong constraint on the day-to-day life and induced changes in the cultural habits on food consumption. Although the first measurements made in the Prefecture were indicating concentration values in foodstuff much lower than those initially expected or announced by different voices, the consumers were generally still reluctant to buy products from Fukushima Prefecture. This confusing situation led us to promote a database providing the available information in order to better inform the residents.

For food on the market, radioactivity measurement results have been published by the Ministry of Health, Labour and Welfare (MHLW) [3], local governments [4, 5], and Japan Agricultural Cooperatives (JA) [6]. As for the foods that residents gathered on kitchen gardens, forests, rivers, and in the sea, the community centers have provided equipment to measure the radiation, etc., so it has become possible to know the amount of radioactivity in food in almost all cases. However, the amount of radioactivity is expressed in Bq/kg, and it is difficult for the local residents to directly estimate the influence of these values on the total dose they

receive (expressed in mSv). In order to determine themselves whether or not to eat the various food products, it is useful to know how much radioactivity they take when they eat those products, the degree of internal exposure, and also the quantity of radioactivity discharged from the body. In this perspective a tool which provides information about all these aspects was considered as very helpful. After the Chernobyl accident, the ETHOS project and the CORE program [7, 8] in the contaminated areas of Belarus provided education for local residents about radiation protection to favor their involvement in their own protection. A software for internal exposure assessment called CORPORE has been developed and used in this program in cooperation with Norwegian radiation protection experts. With this software, it is possible to describe and analyze the results of whole body counters (WBC) measurements. Using this tool allows registering the amount of radioactivity taken during the daily diet and also allows health care workers to open a dialogue with individuals about the radiological quality of the food. By doing so the tool allows to enhance the awareness of residents about the risk of internal exposure and also to help individuals to make informed choices about their diet. Although using this tool to find the cause in the WBC measurement results is a so-called reverse direction, it allows to know how much radioactivity is consumed. The estimate intake of exposure amount taken when people ingest the food is displayed in a graph, which also shows the personal history of the accumulation and discharge of radiation. By using this graph people can decide what is not suitable to eat/suitable to eat sometimes/the amount suitable to eat/occasionally suitable to eat. Finally this approach allows residents to easily be able to determine what to eat.

In this study by using the mechanisms and models of CORPORE taking into consideration the situation in Japan and Japanese eating habits, we implemented and verified our method of internal exposure management and acquiring information about food.

20.2 Methods

The original CORPORE was implemented to respond to the Belarus and Norwegian situation by handling the food products separately and considering two modes of ingestion: chronic intake and episodic intake. Therefore, its use required to be adapted to the typical Japanese environment. Japanese seldom keep eating the same menu everyday. They often eat various dishes using various food products. It is more natural and easy to manage the ingredients rather than dishes for them. Thus, we decided to handle ingestion as dishes for the new system.

Original CORPORE handles only cesium-137 (Cs-137). Other radionuclides were also required to consider in Japan. It was issued for iodine-131 (I-131), cesium-134 (Cs-134), and Cs-137 radioactivity measurements. Although without any details about each food product, the results were also presented for strontium-90(Sr-90) and plutonium measurement on market basket methods [3]. For this reason, it was decided that the support of multi-nuclide is also required. Original CORPORE was

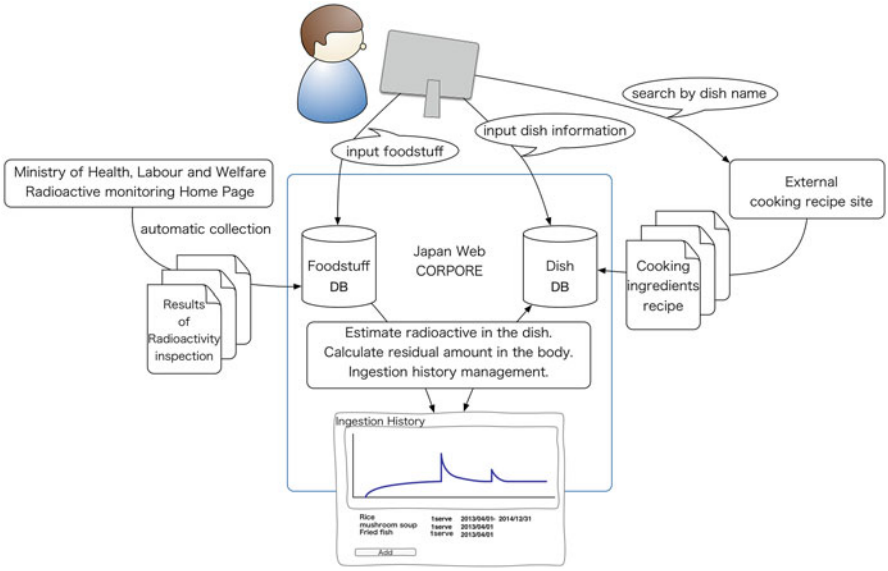

Fig. 20.1 A diagram of Japan Web CORPORE

basically intended for use by radiation protection and medical personnel. In order to be used by residents, the user management system and intake history management system have been developed. Original CORPORE also has statistical functions about the intake status for assessment in order to display the position of the resident in the group. All these features have been kept.

In order to adapt the original CORPORE to the Japanese situation, it is developed as a Web application for widespread use. A database structure allows managing ingestion of food products as dish. It hence supports to various nuclide types. Applying user management function, users can manage their own intake history respectively. To facilitate complicated food information input, food and dish input system is applied so that forward-direction usage can be realized. All these functions are presented in Fig. 20.1 and details are explained below.

20.2.1 System

Local residents can enter their own dish to evaluate their contamination level, so they can make the exposure management of themselves by browsing the radioactivity intake information and internal exposure information. They are also able to access it and use it from personal computers or smart phones through the Internet, as it is developed as a Web application. To operate in typical server configurations, MySQL 5.5 database system, most popular open source database system in the world [9], was

used, and it was implemented in PHP 5.5, Hypertext Preprocessor which is a server-side scripting language [10], to work on typical web server applications such as Apache 2.4 [11], etc. Also, it is available from the general viewing environment, and is successfully displayed in Internet Explorer 9 or higher, Google Chrome version 10.0.648 or higher and Safari version 5.0 or higher.

20.2.2 Database Structure

In order to input food intake situations to match the Japanese food environment, we considered the modification of the food database structure of the original CORPORE. It was initially limited to the food database, and we enlarged it to the ingredients database.

Also, the original CORPORE allowed only Cs-137 input, while in the modified version the database structure corresponds to the multi-radionuclide species. Presented in the survey results by the MHLW released I-131, Cs-134, Sr-90 and plutonium (Pu-238, Pu-239, Pu-240) became a possible input.

20.2.3 Food and Cooking Information Input

Radioactivity test results announced from time to time by the MHLW turn into DB automatically, and this information is available to use for products. As for the food which is ingested daily, by applying the technology developed by Kawashima et al. [12], in cooperation with external recipe information sites, it is possible to avoid the trouble of inputting all the information about materials. Cooking information can be reused as a template.

20.2.4 User Management

To perform user management, the user is enabled to browse his/her intakes in the history of radiation continually and record meals.

In addition, it allows managing the users' rights, such as general user, user with administrative privileges; medical user to make the assessment and research user to make the research were prepared.

The medical user privileges include a privilege to view all the information of the population to perform the individual exposure assessment. The research user privileges include a privilege to view anonymized information about the intake of the population.

20.2.5 Form of Use

Original CORPORE was used in Belarus as an assessment tool (1) to determine the amount of radioactivity in the body using the WBC measurements as inputs, (2) to engage a dialogue with the residents on their diet in case the internal contamination levels were significantly higher than the average level, (3) to analyze the estimated exposure dose using the graph to display it; thus, it is the reverse direction to explore the cause from the result. Displaying the radiation dose that is expected by ingesting the food is not only the opposite direction to determine whether to eat or not. Also, the ingested radioactivity substance amount is recorded, because it is assumed that a possible use of its dose can happen in the future again. This data is saved in history of the daily diet, and it can be displayed in a graph to see the remaining radioactivity quantity in the body.

Moreover, it can be used as an assessment tool, since it matches the functions of the original CORPORE, and in the present system the input and statistics of WBC measurement results are displayed, too.

20.3 Results

In the Web version of CORPORE Japan, it is possible to access the Web application through the Internet, perform user management on the basis of the food ingredients input to make a meal, learn about ingested food information for each user, and display a graph of radioactivity intake and biological half-life discharge status, as well as to be able to confirm oneself the graph of intake and discharge status of radioactivity on the browser. From 0-year-old to 1-year-old, from 2-years-old to 5-years-old, from 6-years-old to 10-years-old, from 11-years-old to 15-years-old the ingested radioactivity is reduced by each of the biological half-life factor by 16-years-old of age or older, and the user's age appearance is displayed as a graph (Fig. 20.2).

As an assessment function, similar to the original CORPORE, it is possible to confirm the statistics display about any users' position among the intake average and make groups of the population on the browser (Fig. 20.3).

Furthermore, the product database is updated periodically through the access to the MHLW website which is obtained automatically, to see the results of the radioactivity tests. In April 2015, about 1.2 million cases of food radioactivity test results were published and are available as contamination information. Although it was confirmed that the database allows entering not only Cs-137 information but also other radionuclides, however, currently this system implemented only Cs-137 biological model, hence the result graphs of such other nuclides are not shown.

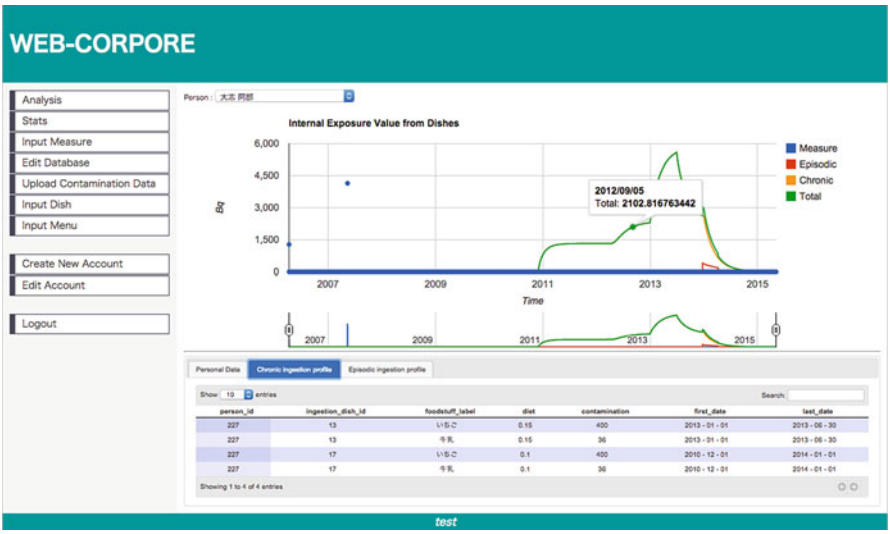

Fig. 20.2 An analysis screen shows the history of radioactivity ingestion and reduction

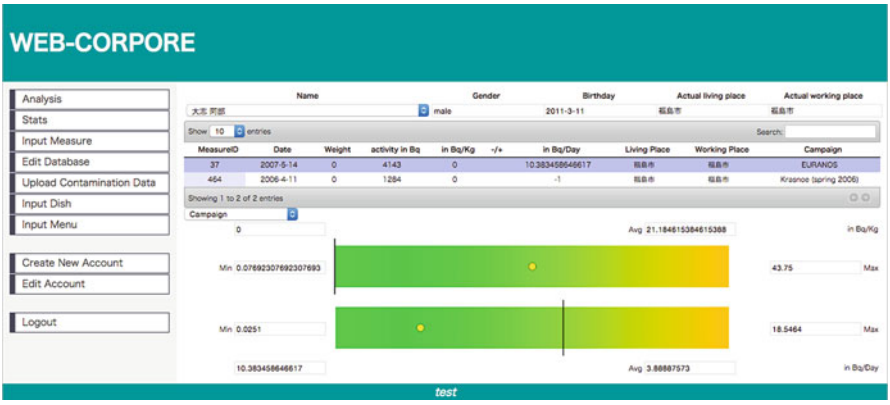

Fig. 20.3 A stats screen shows user's position among the intake average and make groups of the population

20.4 Discussion

20.4.1 Verification of the Usability

As a method of using this system, before cooking any meal or buying any ingredients, one can enter the system from a personal computer or a smart phone, enter the meal ingredients one has access to. By doing this, one will estimate the intake. This way allows obtaining the history of radioactivity intake and estimates

the information about the intake of internal exposure dose, so one can make the decision to reduce the amount to eat/not to eat something if it is not suitable/eat everyday or occasionally/not eat at all/so from that previously ingested data the user can decide what and how much to eat or not. When the user ate it, the information is kept in history and becomes the basic judgment criteria for the meals eaten after. Thus, this system can be considered to contribute to the "recovery of the right to self-determination" and is expected to help residents to regain confidence by managing their day-to-day intakes.

Then, as the present system has been constructed keeping in mind the assessment capabilities of the original CORPORE, it is also applicable for reverse utilized assessment. Therefore, it can be used not only in Japan. In fact, we asked the original CORPORE development team to trial this system, and it was highly evaluated. It was also announced to be easier to use than the "original CORPORE because it is only necessary to input each dish, and not each food ingredient as originally and this is obviously more realistic for the Japanese context," "Because ETHOS and CORE activities in Belarus started 10 years after the accident, Cs-134 was ignored in CORPORE given its very small influence at the start of the project. In Japan, the accident has just happened so the knowledge about short nuclides in their half-life corresponded to the multi-nuclides is extremely valuable."

Also, it became possible to handle the natural origins of radioactivity information from the previous self, and to perform the management of global radioactivity uptake.

The number of food products is 1,199,241, which is integrated in the product database. The levels of 1,113,931 products of them (92.8 %) are under the detection limit value. Among them the number of food products added from January to March 2015 is 67,401, among them 65,117 (96.6 %) are about the detection limit value or less, equal to or greater than the limit value (Table 20.1) of the food makes 145 (0.2 %) of cases. For the 145 ingredients of the limit value or more see Table 20.2. The percentage of foods with the limit value or more is very little, mostly it is wild boar meat, but because black bear meat and Japanese deer meat is not common in a general household it is hardly applicable as a food ingredient for Japan. It can be said that the majority of Japanese people at the moment are hardly affected by this food. However, easy evaluation tools are required in contaminated areas for evaluation and the understanding of the situation. These tools will help to develop the radiation protection culture to individuals allowing them to have a grip on their own protection.

Table 20.1 The reference levels of foods in Japan (Notice No. 0315 Articles 1 of the Department of Food Safety, March 15, 2012)

Category	Limit level (Bq/kg)
Water	10
Soft drinks	10
Tea for drinking	10
Milk	50
Foods other than above	100

Table 20.2 A breakdown of the products positive at levels exceeding limits between January 1st and March 31st 2015 in the product database

Name of product	Number of products positive at levels exceeding limits
Wild boar meat	116
Japanese deer meat	10
Asian black bear meat	5
Copper pheasant meat	3
Japanese stingfish	3
Iwana mountain trout	5
Landlocked masu salmon	1
Mushroom powder	1
Stone flounder	1

Moreover, these tools are urgently required in this situation, and it is essential to prepare and keep them in order in case of future contingencies.

20.4.2 Subject of Future Investigation

The system is made to favor the development of the radiation protection culture of people in contaminated areas and its neighborhoods; it will be one of the tools of reconstruction of their living environment, so it is necessary to consider this system for the future.

This system estimates the amount (Bq) of radioactivity that was ingested by using the mechanism of CORPORE, visualizes the state of users' history, and helps to show the discharged radioactivity as a graph. However, the residents of contaminated areas want to know how much of the exposure dose (mSv) they receive and the ingestion part of it. In the future, it will be necessary to establish a mechanism for displaying the conversion of the level of contamination (Bq) into the internal dose (mSv) by using a conversion coefficient of each species that is provided by the ingested amount of radioactivity of the ICRP Publication 72 [13].

Although inputting cooking information is available and there are cooking information templates to be obtained from a recipe site to make the input easier, it is still a hard work to manage each meal every day. We want to consider the ways to make this process even easier. For example, we consider making it possible to identify food from a photograph of the cooking or the supermarket receipt and POS information of shopping to guess the food.

For determining the amount of the radioactivity ingested, the food eaten by the user might not be available in the food database, and does not correspond to any food measurement results; even if it is unknown it still may be sufficient. We do not consider the radiation level to be 0 but wait a month and build a graph of the uptake potential calculating it from the maximum value and the minimum value of radioactivity in food of the predetermined period on the food database width, or

ingenuity, such as displaying the value of the radioactivity survey conducted before the accident [14]. In this regard we think it is necessary to pursue the reflection on the best way to proceed.

As mentioned earlier, the results for Cs-137 and other nuclide species are not currently integrated into the database structure to correspond to the multi-nuclide variety. This not only concerns nuclides which are listed in the radioactivity measurement results of the MHLW, but also the internal exposure control is possible by ingestion of natural radionuclides by incorporating models such as potassium 40 and polonium 210.

Also, due to the use of a computational model of the original CORPORE calculation system, used in the European context, we would like to consider the comparison method and use of the computational model with accordance to the Japanese data only.

Then, from the original CORPORE development team we receive an opinion that "since the genre of diet became different we want to be able to compare the exposure situations. Separating the diet patterns will help to make groups in the future automatically." For example, seafood diet group, agricultural group, etc. will help to build a kind of patterned templates for further study, and can increase the number of subgroups in each group such as according to gender or regions for future statistical data. In this paper, the system was evaluated by experts. The evaluation by residents is also required to evaluate the actual usability. We intend doing it in the future.

In addition, after the nuclear accident, there was an increasing interest in medical exposure; the efforts have become more active for the medical exposure dose management [15–17]. Also, Dose Structured Report was defined in DICOM as a standard for radiation exposure information management for medical exposure [18], while we are in the environment, which is easy to collect the information of the medical exposure.

As it is described above, in the present situation the influence of internal exposure from food is almost negligible for a large number of individuals although it is of concern for the residents and could be sensitive for specific groups of population consuming home-grown products and products from the forest. The impact of external exposure from the surrounding environment is considered to be potentially larger depending on the area as well as on the individual habits and activities. External exposure data have been gathered in the Prefecture health survey in collaboration with dose assessment [19]. In the future we consider building a system that can manage all the radiation exposures (including medical exposures) of the individual, with the main purpose to develop the radiation protection culture.

In addition, radiation dose information should not only be managed, but also the day-to-day nutrition management and health management could be considered also, with a unification mechanism where individuals can add nutrition information on food. Furthermore, it is expected to be also applicable for the management of the body accumulation of toxics such as arsenic and heavy metals and not only radioactivity.

20.5 Conclusion

Using the tools of the mechanism that has been used for internal exposure assessment in Europe after the Chernobyl nuclear power plant accident, we built a Web application for local residents of contaminated areas suffering from the Fukushima nuclear power plant accident so that they can determine themselves whether or not to eat the food, and use this tool to receive information. The user can input cuisine meals information in food ingredient units in accordance with the Japanese food environment. It is possible to view the quantity of radioactivity ingested and also the history of the internal exposure. It is designed to help to develop the radiation protection culture of residents by capturing the information visually.

Acknowledgement This work was partly funded by the 2012 fiscal year of Education, Culture, Sports, Science and Scientific Research. The results of this study are part of Fukushima Prefecture radiation medicine research and development business subsidy.

References

1. Lochard J et al (2009) ICRP Publication 111 – Application of the Commission's recommendations to the protection of people living in long-term contaminated areas after a nuclear accident or a radiation emergency. Ann ICRP 39(3):1–4, 7–62
2. Clement CH, Sasaki M (2012) The international commission on radiological protection and the accident at the Fukushima nuclear power stations. Jpn J Health Phys 47(3):206–209
3. Ministry of Health, Labor and Welfare (2011) Levels of radioactive contaminants in foods tested in respective prefectures. Available from: http://www.mhlw.go.jp/english/topics/2011eq/index_food_radioactive.html. Accessed Apr 24, 2015
4. Fukushima Prefecture, Monitoring Info (2011). Available from: http://www.new-fukushima.jp/monitoring/en/. Accessed 12 Jul 2015
5. Fukushima city, The result of independent radioactivity inspection of corps in Fukushima city (2011). Available from: http://www.city.fukushima.fukushima.jp/soshiki/22/enngeitokusann12073001.html. Accessed 12 Jul 2015
6. JA Shin Fukushima, Information of radioactivity monitoring (2011). http://www.shinfuku.jp/monita/. Accessed 12 Jul 2015
7. Hériard Dubreuil G et al (1999) Chernobyl post-accident management: the ETHOS project. Health Phys 77(4):361–372
8. Lochard J (2007) Rehabilitation of living conditions in territories contaminated by the Chernobyl accident: the ETHOS project. Health Phys 93(5):522–526
9. MySQL5.5 (2011) http://www.mysql.com/
10. PHPL5.5 (2013) http://php.net/
11. Apache2.4 (2012) http://httpd.apache.org/
12. Kawashima M et al (2015) Development and evaluation of a nutrition management system for elderly people with a dish registration function. IPSJ J 56(1):171–184

13. Japan Chemical Analysis Center (2010) Radioactivity survay data in Japan. 145(Aug 2010)
14. Ota T, Sanada T, Kashiwara Y, Morimoto T, Sato K (2009) Evaluation for committed effective dose due to dietary foods by the intake for Japanese adults. Jpn J Health Phys 44(1):80–88
15. Shannoun F (2015) Medical exposure assessment: the global approach of the United Nations scientific committee on the effects of atomic radiation. Radiat Prot Dosimetry pp. 1–4, doi: 10.1093/rpd/ncv027
16. Rehani MM, Frush DP (2011) Patient exposure tracking: the IAEA smart card project. Radiat Prot Dosim 147(1–2):314–316
17. Takei Y et al (2014) Summary of a survey on radiation exposure during pediatric computed tomography examinations in Japan, focusing on the computed tomography examination environment. Nihon Hoshasen Gijutsu Gakkai Zasshi 70(6):562–568
18. DICOM Standards Committee, WG (2005) Digital Imaging and Communications in Medicine (DICOM). Supplement 94: Diagnostic x-ray radiation dose reporting (dose SR)
19. Akahane K et al (2013) NIRS external dose estimation system for Fukushima residents after the Fukushima Dai-ichi NPP accident. Sci Rep 3:1670